JOC*Article*

Determination of Absolute Configuration Using Density Functional Theory Calculations of Optical Rotation and Electronic Circular Dichroism: Chiral Alkenes

D. M. McCann and P. J. Stephens*

Department of Chemistry, University of Southern California, Los Angeles, California 90089-0482

pstephen@usc.edu

Received April 10, 2006

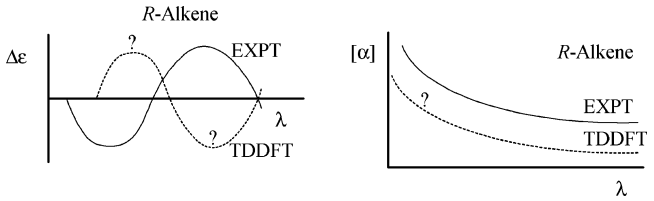

In principle, the absolute configuration (AC) of a chiral molecule can be deduced from its optical rotation (OR) and/or its electronic circular dichroism (ECD). In practice, this requires reliable methodologies for predicting OR and ECD. The recent application of ab initio time-dependent density functional theory (TDDFT) to the calculation of transparent spectral region OR and ECD has greatly enhanced the reliability with which these phenomena can be predicted. TDDFT calculations of OR and ECD are being increasingly utilized in determining ACs. Nevertheless, such calculations are not perfect, and as a result, ACs determined are not 100% reliable. In this paper, we examine the reliability of the TDDFT methods in the case of chiral alkenes. Sodium D line specific rotations, $[\alpha]_D$, are predicted for 26 conformationally rigid alkenes of known AC, ranging in size from 5 to 20 C atoms, and with $[\alpha]_D$ values in the range of 0−500. The mean absolute deviation of predicted $[\alpha]_D$ values from experimental values is 28.7. With one exception, *β*-pinene, the signs of $[\alpha]_D$ are correctly predicted. Errors in calculated $[\alpha]_D$ values are approximately random. Our results define a "zone of indeterminacy" within which calculated $[\alpha]_D$ values cannot be used to determine ACs with >95% confidence. TDDFT ECD spectra are predicted for eight of the alkenes and compared to experimental spectra. Agreement ranges from modestly good to poor, leading to the conclusion that TDDFT calculations of ECD spectra are not yet of sufficient accuracy to routinely provide highly reliable ACs. TDDFT OR calculations for two conformationally flexible alkenes, 3-*tert*-butylcyclohexene and *trans*-4-carene, are also reported. For the former, predicted rotations are incorrect in sign over the range 589−365 nm. It is possible that the AC of this molecule has been incorrectly assigned.

Introduction

The phenomena of optical rotation (OR) and electronic circular dichroism (ECD) have been widely employed for many years in the determination of the absolute configurations (ACs) of chiral molecules.[1] Very recently, the application of the ab initio time-dependent density functional theory (TDDFT) methodology to the calculation of the transparent spectral region OR[2] and the ECD[3] of chiral molecules has greatly enhanced the reliability with which these chiroptical techniques can be predicted and, consequently, their utility in determining ACs.

(1) (a) Djerassi, C. *Optical Rotatory Dispersion, Applications to Organic Chemistry*; McGraw-Hill: New York, 1960. (b) Lightner, D. A.; Gurst, J. E. *Organic Conformational Analysis and Stereochemistry from Circular Dichroism Spectroscopy*; Wiley-VCH: New York, 2000. (c) *Circular Dichroism, Principles and Applications*, 2nd ed.; Berova, N., Nakanishi, K., Woody, R. W., Eds.; Wiley-VCH: New York, 2000.

(2) (a) Cheeseman, J. R.; Frisch, M. J.; Devlin, F. J.; Stephens, P. J. *J. Phys. Chem. A* **2000**, *104*, 1039−1046. (b) Stephens, P. J.; Devlin, F. J.; Cheeseman, J. R.; Frisch, M. J.; Mennucci, B.; Tomasi, J. *Tetrahedron: Asymmetry* **2000**, *11*, 2443−2448. (c) Stephens, P. J.; Devlin, F. J.; Cheeseman, J. R.; Frisch, M. J. *J. Phys. Chem. A* **2001**, *105*, 5356−5371. (d) Mennucci, B.; Tomasi, J.; Cammi, R.; Cheeseman, J. R.; Frisch, M. J.; Devlin, F. J.; Gabriel, S.; Stephens, P. J. *J. Phys. Chem. A* **2002**, *106*, 6102−6113. (e) Grimme, S. *Chem. Phys. Lett.* **2001**, *339*, 380−388. (f) Grimme, S.; Furche, F.; Ahlrichs R. *Chem. Phys. Lett.* **2002**, *361*, 321−328. (g) Autschbach, J.; Patchkovskii, S.; Ziegler, T.; van Gisbergen, S. J. A.; Baerends, E. J. *J. Chem. Phys.* **2002**, *117*, 581−592. (h) Ruud, K.; Helgaker, T. *Chem. Phys. Lett.* **2002**, *352*, 533−539.

10.1021/jo060755+ CCC: $33.50
Published on Web 06/30/2006

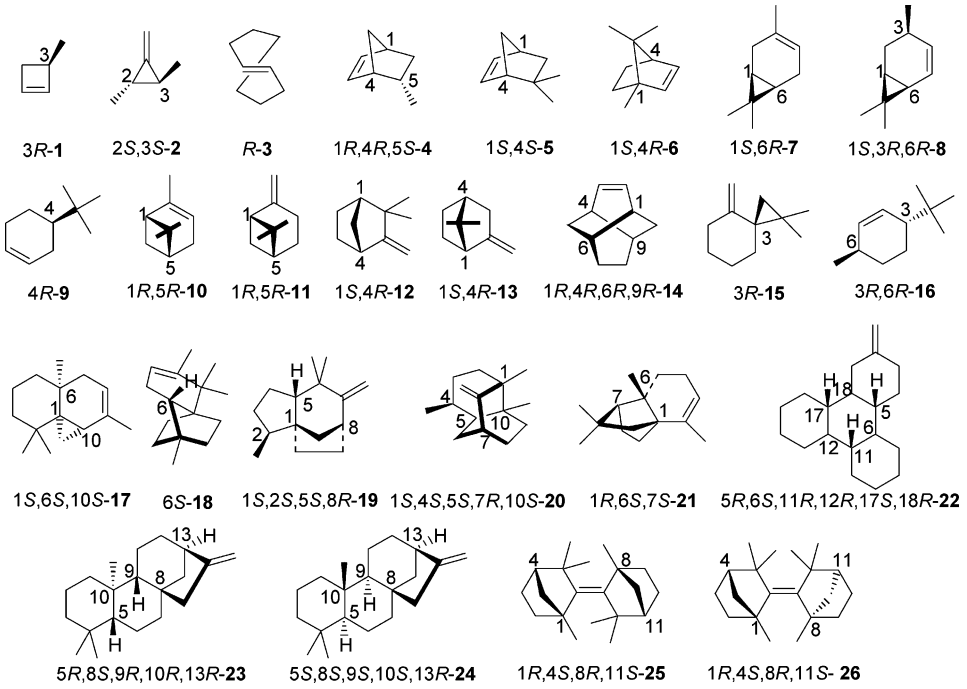

FIGURE 1. Molecules **1**−**26**: **1**, 3-methylcyclobutene; **2**, *trans*-2,3-dimethylmethylenecyclopropane; **3**, *trans*-cyclooctene; **4**, 5-*endo*-methyl-2-norbornene; **5**, camphenilene; **6**, 2-bornene; **7**, 3-carene; **8**, *cis*-4-carene; **9**, 4-*tert*-butylcyclohexene; **10**, α-pinene; **11**, *β*-pinene; **12**, camphene; **13**, α-fenchene; **14**, twistene; **15**, 1,1-dimethyl-4-methylenespiro[2.5]octane; **16**, *trans*-3-*tert*-butyl-6-methylcyclohexene; **17**, thujopsene; **18**, 2,2,3,7-tetramethyltricyclo[5.2.2.0^{1,6}]undec-3-ene; **19**, prezizaene; **20**, seychellene; **21**, neoclovene; **22**, 2-methyleneperhydrotriphenylene; **23**, kaurene; **24**, phyllocladene; **25**, *syn*-(*E*)-bisfenchylidene; **26**, *anti*-(*Z*)-bisfenchylidene.

For a variety of molecules, ACs have been determined using TDDFT calculations of transparent spectral region OR[4] and/or ECD.[5]

In the case of chiral alkanes, the new TDDFT methodology for calculating transparent spectral region OR is of especial value, since ECD is generally at wavelengths too short to be measurable with standard CD instrumentation. In a recent study,[6] we carried out TDDFT OR calculations for a large set of conformationally rigid chiral alkanes to define statistically the reliability of this new methodology. On average, for 21 molecules the deviation between calculated and observed $[\alpha]_D$ values was found to be 24.8. Except for alkanes with small $[\alpha]_D$ values, therefore, TDDFT calculation of transparent spectral region OR should permit ACs to be reliably determined.

In this paper, we extend our study of the new TDDFT methodologies to chiral alkenes. The lowest electronic excitations of alkenes typically occur at substantially longer wavelengths than in the case of alkanes, and their ECD is generally measurable with modern CD instrumentation. However, while substantial literature on the ECD of chiral alkenes does exist,[7] ECD has not been widely used in determining the ACs of alkenes, principally because a reliable sector rule, analogous to the octant rule for the n → π^* transition of carbonyl groups,[8a] has not been available.[8b] As with alkanes, therefore, the new TDDFT methodologies are likely to prove of especial value in determining ACs of chiral alkenes. Here we examine the reliability of TDDFT calculations of the transparent spectral region OR of a large set of conformationally rigid chiral alkenes and simultaneously, for those alkenes for which ECD spectra are available, the reliability of TDDFT calculations of ECD spectra. The molecules chosen for study, **1**−**26**, are shown in Figure 1. As will be demonstrated below, these molecules are conformationally rigid; i.e., at room temperature they exist essentially exclusively in one conformation. This avoids the

(3) (a) Furche, F.; Ahlrichs, R.; Wachsmann, C.; Weber, E.; Sobanski, A.; Vogtle, F.; Grimme, S. *J. Am. Chem. Soc.* **2000**, *122*, 1717−1724. (b) Autschbach, J.; Ziegler, T.; Gisbergen, S. J. A. v.; Baerends, E. J. *J. Chem. Phys.* **2002**, *116*, 6930−6940. (c) Pecul, M.; Ruud, K.; Helgaker, T. *Chem. Phys. Lett.* **2004**, *388*, 110−119.

(4) (a) Stephens, P. J.; Devlin, F. J.; Cheeseman, J. R.; Frisch, M. J.; Rosini, C. *Org. Lett.* **2002**, *4*, 4595−4598. (b) Stephens, P. J.; Devlin, F. J.; Cheeseman, J. R.; Frisch, M. J.; Bortolini, O.; Besse, P. *Chirality* **2003**, *15*, S57−S64. (c) Crassous, J.; Jiang, Z.; Schurig, V.; Polavarapu, P. L. *Tetrahedron: Asymmetry* **2004**, *15*, 1995−2001. (d) Giorgio, E.; Viglione, R. G.; Rosini, C. *Tetrahedron: Asymmetry* **2004**, *15*, 1979−1986. (e) Lattanzi, A.; Viglione, R. G.; Scettri, A.; Zanasi, R. *J. Phys. Chem. A* **2004**, *108*, 10749−10753. (f) McCann, D. M.; Stephens, P. J.; Cheeseman, J. R. *J. Org. Chem.* **2004**, *69*, 8709−8717. (g) Stephens, P. J.; McCann, D. M.; Devlin, F. J.; Cheeseman, J. R.; Frisch, M. J. *J. Am. Chem. Soc.* **2004**, *126*, 7514−7521. (h) Stephens, P. J.; McCann, D. M.; Butkus, E.; Stoncius, S.; Cheeseman, J. R.; Frisch, M. J. *J. Org. Chem.* **2004**, *69*, 1948−1958. (i) Giorgio, E.; Maddau, L.; Spanu, E.; Evidente, A.; Rosini, C. *J. Org. Chem.* **2005**, *70*, 7−13. (j) Giorgio, E.; Roje, M.; Tanaka, K.; Hamersak, Z.; Nakanishi, K.; Rosini, C.; Berova, N. *J. Org. Chem.* **2005**, *70*, 6557−6563. (k) Petrovic, A.; Polavarapu, P. L.; Drabowicz, J.; Zhang, Y.; McConnell, O. J.; Duddeck, H. *Chem. Eur. J.* **2005**, *14*, 4257−4262. (l) Petrovic, A. G.; He, J.; Polavarapu, P. L.; Xiao, L. S.; Armstrong, D. W. *Org. Biomol. Chem.* **2005**, *3*, 1977−1981. (m) Stephens, P. J.; McCann, D. M.; Cheeseman, J. R.; Frisch, M. J. *Chirality* **2005**, *17*, S52−S64. (n) Cheng, M.; Li, Q.; Lin, B.; Sha, Y.; Ren, J.; He, Y.; Wang, Q.; Hua, H.; Ruud, K. *Tetrahedron: Asymmetry* **2006**, *17*, 179−183.

(5) (a) Wang, Y.; Raabe, G.; Repges, C.; Fleischhauer, J. *Int. J. Quantum Chem.* **2003**, *93*, 265−270. (b) Braun, M.; Hohmann, A.; Rahematpura, J.; Bühne, C.; Grimme, S. *Chem.—Eur. J.* **2004**, *10*, 4584−4593. (c) Reference 4g. (d) Reference 4h. (e) Schühly, W.; Crockett, S. L.; Fabian, W. M. F. *Chirality* **2005**, *17*, 250−256.

(6) McCann, D. M.; Stephens, P. J.; Cheeseman, J. R. *J. Org. Chem.* **2004**, *69*, 8709−8717.

(7) See, for example: (a) Scott, A. I.; Wrixon, A. D. *Tetrahedron* **1970**, *26*, 3695−3715. (b) Scott, A. I.; Wrixon, A. D. *Tetrahedron* **1971**, *27*, 4787−4819. (c) Hudec, J.; Kirk, D. N. *Tetrahedron* **1976**, *32*, 2475−2506. (d) Drake, A. F.; Mason, S. F. *Tetrahedron* **1977**, *33*, 937−949.

(8) (a) Reference 1b, Chapter 4. (b) Reference 1b, Chapter 12.

complications which ensue in the case of conformationally flexible molecules.[4b] They range in size from **1**, containing 5 C atoms, to the diterpenes **23** and **24**, containing 20 C atoms. For all molecules, sodium D line specific rotations, $[\alpha]_D$, have been reported and ACs have been assigned. For eight of these molecules, ECD spectra are also available. Our results provide the first statistically significant evaluation of the reliability of the new TDDFT techniques in determining the ACs of chiral alkenes.

In addition to the 26 conformationally rigid alkenes **1**−**26**, we have further predicted the specific rotations of two conformationally flexible chiral alkenes, 3-*tert*-butylcyclohexene, **28**, and *trans*-4-carene, **29**. Our results for these molecules provide specific examples of additional issues which arise in utilizing TDDFT/GIAO calculations of specific rotations in determining ACs of conformationally flexible molecules.

Methods

Conformational analysis of molecules **1**−**26**, **28**, and **29** has been carried out as follows. Initially, stable conformations are identified via Monte Carlo searching with the MMFF94 molecular mechanics force field using the SPARTAN 02 program.[9] All conformations resulting are then reoptimized using DFT at the B3LYP/6-31G* level using the GAUSSIAN 03 program.[10] For all conformations, B3LYP/6-31G* harmonic vibrational frequencies are then calculated to confirm their stability. Finally, conformational free energies are calculated. In some cases, to confirm the completeness of the conformational analysis, additional scans of the potential energy surface (PES) with respect to selected dihedral angles are carried out and/or additional structures are built and optimized at the B3LYP/6-31G* level.

The electric dipole−magnetic dipole polarizabilities at wavelength λ, $\beta_{\alpha\beta}(\lambda)$, and thence the specific rotations, $[\alpha]_\lambda$, of stable conformations of **1**−**26**, **28**, and **29** are then calculated using the TDDFT/GIAO methodology of Cheeseman, Frisch, and Stephens, implemented in GAUSSIAN 03, as detailed in prior papers.[2a−d,4a,b,f−h,m] We emphasize that the use of GIAOs leads to origin-independent values of $\beta = \mathrm{Tr}[\beta_{\alpha\beta}]$ and, thence, $[\alpha]$, in contrast to TDDFT methodologies, which do not use GIAOs and lead to origin-dependent values of β and $[\alpha]$.[2a] Of course, *calculated [α] values can only be meaningfully compared to experimental values when they are origin-independent*. Calculations of β and $[\alpha]$ are carried out using basis sets containing diffuse functions, which have been shown to be essential in minimizing basis set error for these properties.[2a,c,e−g] Specifically, as in prior work,[2a−d,4a,b,f−h,m] we have used the aug-cc-pVDZ and 6-311++G(2d,2p) basis sets, which provide an acceptable compromise between computational labor and basis set error.[2a,c] The state-of-the-art hybrid density functionals B3LYP, B3PW91, and PBE1PBE have been used, as in prior work.[2a−d,4a,b,f−h,m] Calculations have been carried out using B3LYP/6-31G* equilibrium geometries and, in some cases, geometries optimized using other ab initio methods.

The energies, oscillator strengths, and rotational strengths of the electronic excitations of molecules **3**, **6**, **10**−**12**, **14**, **24**, and **25** have been calculated using the TDDFT methodology of GAUSSIAN 03, as detailed in prior papers.[5c,d] Rotational strengths are calculated using both length and velocity representations. In the absence of GIAOs, these are origin-dependent and origin-independent, respectively. In comparing calculated ECD spectra to experimental spectra, we use only the origin-independent velocity rotational strengths. However, since length and velocity rotational strengths converge to the same value in the complete basis set limit, the calculation of both enables the convergence to this limit of the finite basis sets we use to be gauged. For consistency, the same basis sets, functionals, and equilibrium geometries are used as for specific rotation calculations.

Electronic excitation energies and rotational strengths are calculated for vertical excitations at ground-state equilibrium geometries. ECD spectra are obtained thence assuming the Condon approximation and, in the absence at this time of a practicable DFT methodology for computing the band shapes of electronic transitions, assuming Gaussian band shapes.[75]

Results

The experimental specific rotations, $[\alpha]_D$, for molecules **1**−**26** are summarized in Table 1, together with their reported ACs. For some molecules enantiomeric excesses (ee's) were determined simultaneously, enabling $[\alpha]_D$ values in the limit of optical purity to be obtained, as also detailed in Table 1. Most ACs have been determined by chemical correlation, i.e., by connection using reactions of predictable stereochemistry to other molecules of known AC. A useful compendium of ACs determined by chemical correlation is ref 35.

Optically active 3-methylcyclobutene, **1**, was first synthesized by Rossi and Diversi.[11] (+)-**1** with $[\alpha]_D = +116.24$ (neat) was shown to have the *R* AC and to be of minimum optical purity 66.2% by oxidation to methylsuccinic acid.

Optically active *trans*-2,3-dimethylmethylenecyclopropane, **2**, was first synthesized by Gajewski from Feist's acid.[12] The AC follows from that of Feist's acid. The most chemically pure sample gave $[\alpha]_D = -57.6$ (CCl_4). Its ee was not reported.

(9) *Spartan 02*; Wavefunction Inc.: Irvine, CA.
(10) *Gaussian 03*; Gaussian, Inc.: Wallingford, CT.

(11) Rossi, R.; Diversi, P. *Tetrahedron* **1970**, *26*, 5033−5039.
(12) Gajewski, J. J. *J. Am. Chem. Soc.* **1971**, *93*, 4450−4458.
(13) (a) Cope, A. C.; Ganellin, C. R.; Johnson, H. W.; Van Auken, T. V.; Winkler, H. J. S. *J. Am. Chem. Soc.* **1963**, *85*, 3276−3279. (b) Corey, E. J.; Shulman, J. I. *Tetrahedron Lett.* **1968**, 3655−3658.
(14) Berson, J. A.; Walia, J. S.; Remanick, A.; Suzuki, S.; Reynolds-Warnhoff, P.; Willner, D. *J. Am. Chem. Soc.* **1961**, *83*, 3986−3997.
(15) Suzuki, A.; Miki, M.; Itoh, M. *Tetrahedron* **1967**, *23*, 3621−3629.
(16) Jadhav, P. K.; Prasad, J. V. N. V.; Brown, H. C. *J. Org. Chem.* **1985**, *50*, 3203−3206.
(17) Gollnick, G. *Tetrahedron Lett.* **1966**, *3*, 327−333.
(18) Bellucci, G.; Ingrosso, G.; Marsili, A.; Mastrorilli, E.; Morelli, I. *J. Org. Chem.* **1977**, *42*, 1079−1081.
(19) Brown, H. C.; Jadhav, P. K.; Desai, M. C. *J. Org. Chem.* **1982**, *47*, 4583−4584.
(20) Brown, H. C.; Zaidlewicz, M.; Bhat, K. S. *J. Org. Chem.* **1989**, *54*, 1764−1766.
(21) Biellmann, J.-F.; d'Orchymont, H *J. Org. Chem.* **1982**, *47*, 2882−2886.
(22) Kokke, W. C. M. C. *J. Org. Chem.* **1973**, *38*, 2989−2994.
(23) Tichy, M. *Collect. Czech. Chem. Commun.* **1974**, *39*, 2673−2684.
(24) Johnson, C. R.; Barbachyn, M, R. *J. Am. Chem. Soc.* **1982**, *104*, 4290−4291.
(25) Norin, T. *Acta Chem. Scand.* **1961**, *15*, 1676−1694.
(26) Daeniker, H. U.; Hochstetler, A. R.; Kaiser, K.; Kitchens, G. C. *J. Org. Chem.* **1972**, *37*, 1−5.
(27) Anderson, N. H.; Falcone, M. S. *Chem. Ind. (London)* **1971**, 62−63.
(28) Wolff, G.; Ourisson, G. *Tetrahedron* **1969**, *25*, 4903−4914.
(29) (a) Parker, W.; Raphael, R. A.; Roberts, J. S. *Tetrahedron Lett.* **1965,** 2313−2316. (b) Parker, W.; Raphael, R. A.; Roberts, J. S. *J. Chem. Soc. C* **1969**, 2634−2643.
(30) Farina, M.; Audisio, G. *Tetrahedron* **1970**, *26*, 1839−1844.
(31) Appleton, R. A.; Gunn, P. A.; McCrindle, R. *J. Chem. Soc. C* **1970**, 1148−1152.
(32) Perry, N. B.; Weavers, R. T. *Phytochemistry* **1985**, *24*, 2899−2904.
(33) Back, T. G.; Barton, D. H. R.; Britten-Kelly, M. R.; Guziec, F. A. *J. Chem. Soc., Perkin Trans. 1* **1976**, 2079−2089.
(34) Brooks, P. R.; Bishop, R.; Counter, J. A.; Tiekink, E. R. T. *J. Org. Chem.* **1994**, *59*, 1365−1368.
(35) Klyne, W.; Buckingham, J. *Atlas of Stereochemistry: Absolute Configurations of Organic Molecules*; Oxford University Press: New York, 1974.

TABLE 1. Experimental and Calculated Specific Rotations of Alkenes 1−26

molecule	ref	AC	$[\alpha]_D$(exptl)[a]	ee (%)	$[\alpha]_D$(exptl)[a] (100% ee)	solvent	concn[c]	$[\alpha]_D$(calcd)[a,b]
1	11	3*R*	116.24	≥66.2	≤175.59	neat		171.6
2	12	2*S*,3*S*	−57.6			CCl_4	1.72	−4.5
3	13	*R*	−426	100	−426	CH_2Cl_2	0.41	−411.7
4	14	1*R*,4*R*,5*S*		100	−90.2	$CHCl_3$	8.95	−117.4
5	14	1*S*,4*S*		100	−48.7	C_6H_6		−83.5
6	15	1*S*,4*R*	−22.43			C_6H_6	3.1	−25.0
7	16	1*S*,6*R*	17.7	100	17.7	neat		31.9
8	17	1*S*,3*R*,6*R*	−161.56			C_6H_6		−184.2
9	18	4*R*	82.8			$CHCl_3$		54.1
10	19	1*R*,5*R*	51.6	100	51.6	neat		41.8
11	20	1*R*,5*R*	23.1	100	23.1	neat		−26.1
12	21	1*S*,4*R*	−107.7	92	−117.1	C_6H_6	5.4	−126.9
13	22	1*S*,4*R*	−42.62	90.7	−46.99	ethyl acetate		−36.6
14	23	1*R*,4*R*,6*R*,9*R*	416.9	100	416.9	EtOH	0.4	361.8
15	24	3*R*	−32.1			$CHCl_3$	1.01	−12.2
16	18	3*R*,6*R*	117.6	100	117.6	$CHCl_3$	6	212.1
17	25	1*S*,6*S*,10*S*	−110			$CHCl_3$	2	−135.1
18	26	6*S*	−64			neat		−65.1
19	27	1*S*,2*S*,5*S*,8*R*	55			MeOH	0.02	54.2
20	28	1*S*,4*S*,5*S*,7*R*,10*S*	−72			$CHCl_3$	0.4	−87.1
21	29	1*R*,6*S*,7*S*	−72.0			$CHCl_3$	1.78	−88.8
22	30	5*R*,6*S*,11*R*,12*R*,17*S*,18*R*	63	53.7	117	$CHCl_3$		73.4
23	31	5*R*,8*S*,9*R*,10*R*,13*R*	−78			$CHCl_3$	0.5−1	−129.7
24	32	5*S*,8*S*,9*S*,10*S*,13*R*	18			$CHCl_3$		1.2
25	33	1*R*,4*S*,8*R*,11*S*	−240.0			EtOH	0.3	−188.9
26	34	1*R*,4*S*,8*R*,11*S*	−206			EtOH	0.57	−279.6

[a] $[\alpha]_D$ in deg $[dm \cdot g/cm^3]^{-1}$. [b] B3LYP/aug-cc-pVDZ//B3LYP/6-31G*. [c] Concentrations in g/100 mL.

Optically active *trans*-cyclooctene, **3**, was first obtained by Cope et al. via resolution of *trans*-dichloro-*trans*-cyclooctene-α-methylbenzylamineplatinum(II), **27**, by means of fractional crystallization.[13a] Its AC was first assigned as *S*-(−) by Moscowitz and Mislow on the basis of semiempirical calculations.[36] Subsequently, Cope and Mehta obtained the AC *R*-(−) by conversion of **3** to *trans*-1,2-dimethoxycyclooctane.[37] The *R*-(−) AC was further confirmed by Manor et al. via X-ray crystallography of **27**.[38] The optical purity of the (−)-**3** of Cope et al.[13a] was subsequently demonstrated by Corey and Shulman.[13b]

The maximum rotations of optically active 5-*endo*-methyl-2-norbornene, **4**, and camphenilene, **5**, were determined by Berson et al.[14] Their ACs were obtained by chemical correlation.

The monoterpene 2-bornene, **6**, is naturally occurring.[39] Its $[\alpha]_D$ has been reported many times.[40] We have not found ee values, which are presumably close to 100% for the highest rotations. Its AC has been established by chemical correlation.[41]

The monoterpene 3-carene, **7**, is naturally occurring.[39] Its AC has been established by chemical correlation.[42] The $[\alpha]_D$ of optically pure **7** has been established by Brown and co-workers.[16] The monoterpene *cis*-4-carene, **8**, is obtained from 3-carene.[39] Its AC has been obtained by chemical correlation.[43] Its ee was not reported.

Optically active 4-*tert*-butylcyclohexene, **9**, was synthesized from *cis*-3-*tert*-butylcyclohexanol of known AC by Bellucci et al.[18] Its ee was not reported. Optically active *trans*-3-*tert*-butyl-6-methylcyclohexene, **16**, was also obtained by these authors from optically pure pulegone of known AC and expected to be optically pure.

The monoterpenes α-pinene, **10**, and *β*-pinene, **11**, are naturally occurring.[39] Their ACs have been established by chemical correlation.[44] The $[\alpha]_D$ values of optically pure **10** and **11** have been established by Brown and co-workers.[19,20]

The monoterpene camphene, **12**, is naturally occurring.[39] Its AC has been established by chemical correlation.[45] The AC of the monoterpene α-fenchene, **13**, has been established by chemical correlation.[46]

The gyrochiral alkene twistene, **14**, was first synthesized in optically active form by Tichy and Sicher.[47] Its AC was assigned via conversion to 4-twistanone, whose AC was obtained from its n → *π** carbonyl group Cotton effect using the octant rule.[8a] The latter AC was subsequently shown by Tichy[23] to be incorrect by synthesis from precursors of known AC, requiring reversal of the AC of **14**. The ee of **14** was established by conversion to twistane of known optical purity.[23]

Molecule **15** was first synthesized in optically active form by Johnson and Barbachyn.[24] Its ee was not reported.

The sesquiterpene thujopsene, **17**, is naturally occurring. Its AC was first established by Norin,[25,48] via correlation with ketones whose ACs were determined from their ORD using the octant rule.[8a] Ee's have not been reported. The sesquiterpene, **18**, was obtained by acid-catalyzed rearrangement of **17** and structurally characterized by Dauben and Friedrich.[49] The AC was based on the known AC of **17**. Ee's have not been reported.

The sesquiterpene prezizaene, **19**, was first isolated and

(36) Moscowitz, A.; Mislow, K. *J. Am. Chem. Soc.* **1962**, *84*, 4605−4606.
(37) Cope, A. C.; Mehta, A. S. *J. Am. Chem. Soc.* **1964**, *86*, 5626−5630.
(38) Manor, P. C.; Shoemaker, D. P.; Parkes, A. J. *J. Am. Chem. Soc.* **1970**, *92*, 5260−5262.
(39) Erman, W. F. *Chemistry of the Monoterpenes*; Marcel Dekker Inc.: New York, 1985.
(40) *Crossfire Beilstein Database*; MDL Information Systems GmbH: Frankfurt, Germany, 2005.
(41) Reference 39, Chapter 3.
(42) Reference 35, p 39. Reference 39, Chapter 3.
(43) Reference 35, p 82. Reference 39, Chapter 3.
(44) Reference 35, pp 84 and 87. Reference 39, Chapter 3.
(45) Reference 35, p 87. Reference 39, Chapter 3.
(46) Reference 35, p 86. Reference 39, Chapter 3.
(47) Tichy, M.; Sicher, J. *Tetrahedron Lett.* **1969**, 4609−4613.
(48) Norin, T. *Acta Chem. Scand.* **1963**, *17*, 738−748.
(49) Dauben, W. G.; Friedrich, L. E. *J. Org. Chem.* **1972**, *37*, 241−250.

TABLE 2. Conformational Analysis of Alkenes 3, 9, 15−17, 20, 22−24, 28, and 29[a]

molecule	conf[b]	$\Delta E^{c,d}$	$\Delta E^{c,e}$	$\Delta G^{c,e}$		molecule	conf[b]	$\Delta E^{c,d}$	$\Delta E^{c,e}$	$\Delta G^{c,e}$
3	**a**	0.00	0.00	0.00	**a**	**22**[h]	CCCC	0.00	0.00	0.00
	b	2.40	5.66	4.75	**b**		CCCB	4.71	5.23	5.26
	d	6.98					CCBC	4.71	5.15	5.37
	c	4.65	5.96	5.64	**c**		BCCC	4.82	4.46	4.44
	e	8.39					CCBB	9.92	10.85	10.90
							BCBC	10.01	10.08	9.99
9	**a**	0.00	0.00	0.00			BCCB	10.02	10.22	9.98
	b	4.25	3.76	3.87			BCBB	15.51	16.29	15.67
15	C	0.00	0.00	0.00		**23**[i]	CCC	0.00	0.00	0.00
	C	2.36	2.77	3.02			BCC	2.65	2.98	3.49
	B	5.83	5.10	4.57			CBB	5.72	5.51	4.71
	B	5.98	4.90	4.42			BBB	11.53	10.72	10.07
	B	6.21	5.24	4.91			BBB	12.31	10.89	10.70
	B	6.59	6.86	6.77			BBB	12.68	12.48	11.92
							BBC	13.00	12.59	12.60
16	**a**	0.00	0.00	0.00						
	b	2.48	2.48	2.63		**24**[i]	CCC	0.00	0.00	0.00
							BCC	3.26	3.47	3.69
17[f]	C	0.00	0.00	0.00			CBC	10.37	8.18	8.46
	B	2.27	5.09	4.95			BBC	13.72	11.47	11.91
	B	3.68	5.64	5.38						
	C	3.72	5.49	5.86		**28**	**a**	0.00	0.00	0.00
	B	3.89	3.15	3.58			**b**	2.11	1.65	1.73
	B	4.03	6.26	6.26						
						29	**a**	*j*	0.00	0.00
20[g]	C	0.00	0.00	0.00			**b**	*j*	0.64	0.56
	B	12.72	9.96	10.23						

[a] See the Supporting Information, Figure 1 and Table 1, for a more detailed description of the conformations of **3**, **9**, **15**−**17**, **20**, **22**−**24**, **28**, and **29**. [b] C = chair, and B = boat. [c] Units of kcal/mol. [d] MMFF94. [e] B3LYP/6-31G*. [f] Conformations of ring C1C2C3C4C5C6. [g] Conformations of ring C1C2C3C4C5C10. [h] Conformations of rings C1C2C3C4C5C18, C5C6C11C12C17C18, C6C7C8C9C10C11, and C12C13C14C15C16C17. [i] Conformations of rings C1C2C3C4C5C10, C5C6C7C8C9C10, and C8C9C11C12C13C14. [j] Only one conformation predicted by MMFF94.

structurally characterized by Anderson and Falcone.[27] The AC was confirmed by the CD of the ketone obtained on conversion of the *exo*-methylene group to a carbonyl group, together with the octant rule.[8a] The ee was not reported.

The sesquiterpene seychellene, **20**, was isolated and structurally characterized by Wolff and Ourisson.[28] Its AC was established by correlation with the ketones norseychellanone and 4a,5,8-trimethyloctahydronaphthalen-2-one, whose ACs were determined via their CD spectra, using the octant rule.[8a] The ee was not reported.

The sesquiterpene neoclovene, **21**, was first obtained by Raphael and co-workers[29] by acid rearrangement of caryophyllene. Its AC was deduced from that of caryophyllene and from those of the ketones 4-isopropyl-3,3-dimethylcyclohexanone and 6,8,8-tetramethyltricyclo[5.2.2.$0^{1,6}$]undecan-3-one, whose ACs were determined from their ORD curves using the octant rule.[8a] Neoclovene was subsequently shown to be naturally occurring and renamed α-neoclovene.[50] Ee values do not appear to have been determined.

2-Methyleneperhydrotriphenylene, **22**, was first synthesized in optically active form by Farina and Audisio[30] from the 2-COOH derivative of *anti-trans-anti-trans-anti-trans*-perhydrotriphenylene (PHTP). Its AC was determined by conversion to the 2-CO derivative of PHTP, whose AC was determined from its ORD and CD using the octant rule.[8a] The ee of the precursor acid was determined, enabling the $[\alpha]_D$ of optically pure **22** to be obtained.

The isomeric diterpenes kaurene, **23**, and phyllocladene, **24**, are naturally occurring. Their ACs have been established by chemical correlation.[51] Specific rotations have been reported without ee values.

The *syn-E* isomer of bisfenchylidene, **25**, was first synthesized by Barton and co-workers[33] from fenchone. The *anti-Z* isomer, **26**, was subsequently also isolated by Brooks et al.[34] The ACs of **25** and **26** derive from that of fenchone. Ee's were not reported.

Before calculation of the $[\alpha]_D$ values of **1**−**26**, it is necessary to obtain their equilibrium structures and, in the case of molecules which are conformationally flexible, to verify that only one conformation is significantly populated at room temperature. For all molecules, we have initially carried out a Monte Carlo conformational search using the MMFF94 molecular mechanics force field to define the structures and relative energies of the possible conformations. The MMFF94 structures obtained are reoptimized using DFT at the B3LYP/6-31G* level to obtain the B3LYP/6-31G* structures and relative energies of all conformations. B3LYP/6-31G* harmonic vibrational frequencies are then calculated to confirm the stability of all conformations and to permit the calculation of their relative free energies. The molecule is defined as "conformationally rigid" if there are no conformations whose B3LYP/6-31G* free energies are within 2 kcal/mol of the lowest energy conformation. Where more than one conformation is found, MMFF94 and B3LYP/6-31G* relative energies and B3LYP/6-31G* relative free energies are given in Table 2. All molecules **1**−**26** are predicted to be rigid.

In the case of **3**, both MMFF94 and B3LYP/6-31G* predict that the conformation of lowest energy is the C_2-symmetry crown/twist conformation. Structural parameters obtained by

(50) Yoshihara, K.; Hirose, Y. *Bull. Chem. Soc. Jpn.* **1975**, *48*, 2078−2080.

(51) Reference 35, pp 109 and 112.

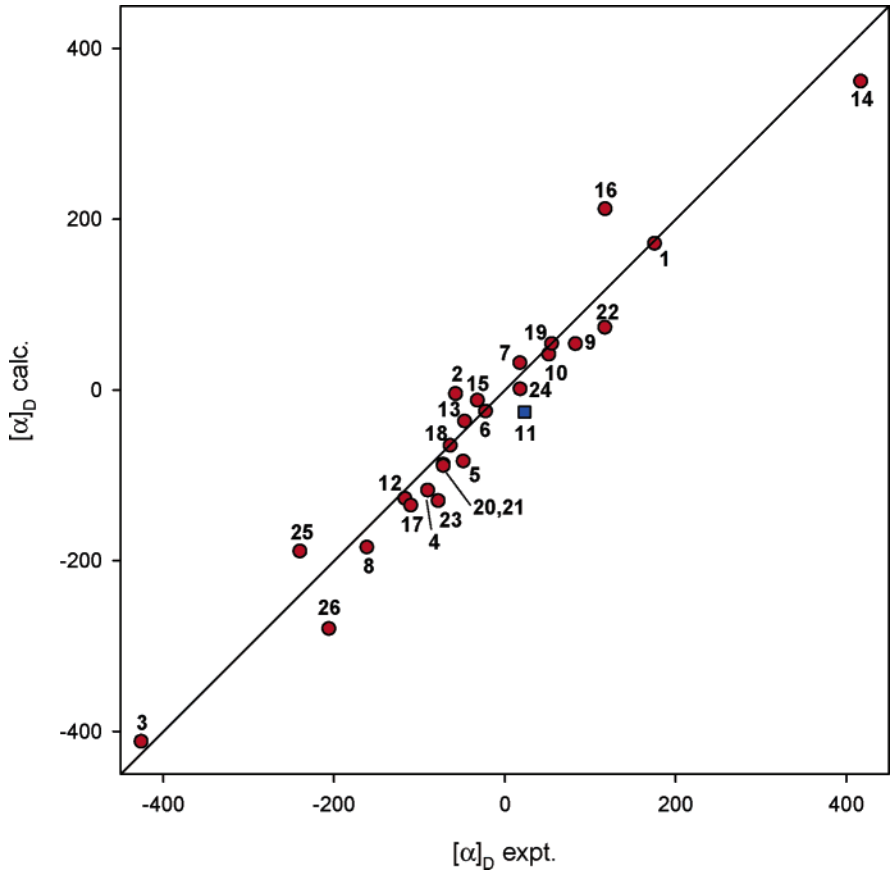

FIGURE 2. Comparison of calculated and experimental $[\alpha]_D$ values of **1**−**26**. The line has slope +1. The blue square indicates that the calculated $[\alpha]_D$ is erroneous in sign.

electron diffraction[52] are compared to the corresponding predicted parameters in Table 1 of the Supporting Information (SI). Agreement is good for both MMFF94 and B3LYP/6-31G* structures. MMFF94 predicts four higher energy conformations, two (**b** and **d**) of C_2 symmetry and two (**c** and **e**) of C_1 symmetry. B3LYP/6-31G* optimization of these structures reduces the number of conformations to two, one of C_2 symmetry (**b**) and one of C_1 symmetry (**c**). Structural parameters for the MMFF94 conformations **b**−**e** and the B3LYP/6-31G* conformations **b** and **c** are also given in Table 1 of the SI. The structures of all conformations are illustrated in Figure 1 of the SI.

In the cases of **7** and **8**, only one conformation is predicted by MMFF94. To confirm that the cyclohexene rings have only one conformation at the B3LYP/6-31G* level, the potential energy surfaces of **7** and **8** have been scanned as a function of the dihedral angles C3C4C5C6 and C1C2C3C4, respectively, with the results shown in Figures 2 and 3 of the SI. No additional minima are found, confirming the rigidity of the cyclohexene rings.

In the cases of **9** and **16**, two conformations are predicted, having oppositely puckered rings. The structures are shown in Figure 4 of the SI; the ring dihedral angles are given in Table 2 of the SI.

In the case of **15**, remarkably, six distinct conformations are predicted. Their structures are shown in Figure 1 of the SI. In the case of **17**, six distinct conformations are predicted. Their structures are shown in Figure 1 of the SI. In the case of **18**, only one conformation is predicted by MMFF94.

In the case of **19**, only one conformation is predicted by MMFF94. To confirm that the cyclopentane ring has only one conformation at the B3LYP/6-31G* level, we have scanned the PES with respect to the dihedral angle C1C5C4C3, with the results shown in Figure 5 of the SI. No additional minima are found, confirming the rigidity of the cyclopentane ring.

In the case of **20**, two conformations are predicted. Their structures are shown in Figure 1 of the SI.

In the case of **21**, only one conformation is predicted by MMFF94. To confirm that the cyclohexene ring has only one conformation at the B3LYP/6-31G* level, we have scanned the PES with respect to the dihedral angle C1C6C5C4, with the results shown in Figure 6 of the SI. No additional minima are found, confirming the rigidity of the cyclohexene ring.

In the case of **22**, eight conformations are predicted. Their structures are shown in Figure 1 of the SI. In the cases of **23** and **24**, seven and four conformations are predicted, respectively. Their structures are shown in Figure 1 of the SI.

The bisfenchylidenes **25** and **26** are conformationally rigid. X-ray structures have been reported for these molecules.[65,66] Bond lengths, bond angles, and dihedral angles of our B3LYP/6-31G* geometries and the X-ray structures are compared in Table 3 of the SI. Agreement is excellent.

TDDFT/GIAO $[\alpha]_D$ values calculated at the B3LYP/6-31G* equilibrium geometries of the lowest energy conformations of **1**−**26** using the functional B3LYP and the aug-cc-pVDZ basis set are given in Table 1 and compared to experimental $[\alpha]_D$

(52) Trætteberg, M. *Acta Chem. Scand., B* **1975**, *29*, 29−36.

TABLE 3. Dependence of Calculated $[\alpha]_D$ Values for Alkenes 3, 10, and 11 on the Density Functional, Basis Set, and Equilibrium Geometry

molecule	geometry	functional	basis set	$[\alpha]_D$
(*R*)-**3**	B3LYP/6-31G*	B3LYP	aug-cc-pVDZ	−411.7
	B3LYP/6-31G*	B3PW91	aug-cc-pVDZ	−393.3
	B3LYP/6-31G*	PBE1PBE	aug-cc-pVDZ	−403.5
	B3LYP/6-31G*	B3LYP	6-311++G(2d,2p)	−404.1
	MP2/6-31G*	B3LYP	aug-cc-pVDZ	−468.9
	B3LYP/TZ2P	B3LYP	aug-cc-pVDZ	−406.1
	B3LYP/cc-pVTZ	B3LYP	aug-cc-pVDZ	−407.9
	HF/6-31G*	B3LYP	aug-cc-pVDZ	−386.7
(1*R*,5*R*)-**10**	B3LYP/6-31G*	B3LYP	aug-cc-pVDZ	41.8
	B3LYP/6-31G*	B3PW91	aug-cc-pVDZ	49.5
	B3LYP/6-31G*	PBE1PBE	aug-cc-pVDZ	45.5
	B3LYP/6-31G*	B3LYP	6-311++G(2d,2p)	36.9
	B3LYP/SVP	B3LYP	aug-cc-pVDZ	42.3
	MP2/6-31G*	B3LYP	aug-cc-pVDZ	42.6
	B3LYP/TZ2P	B3LYP	aug-cc-pVDZ	44.0
	HF/6-31G*	B3LYP	aug-cc-pVDZ	43.1
(1*R*,5*R*)-**11**	B3LYP/6-31G*	B3LYP	aug-cc-pVDZ	−26.1
	B3LYP/6-31G*	B3PW91	aug-cc-pVDZ	−18.9
	B3LYP/6-31G*	PBE1PBE	aug-cc-pVDZ	−17.2
	B3LYP/6-31G*	B3LYP	6-311++G(2d,2p)	−26.9
	B3LYP/SVP	B3LYP	aug-cc-pVDZ	−23.8
	MP2/6-31G*	B3LYP	aug-cc-pVDZ	−17.3
	B3LYP/TZ2P	B3LYP	aug-cc-pVDZ	−26.7
	HF/6-31G*	B3LYP	aug-cc-pVDZ	−18.4

values in Figure 2. Qualitatively, the overall correlation of calculated and experimental $[\alpha]_D$ values is very good. Quantitatively, experimental $[\alpha]_D$ values range from −426 to +416.9. Differences of calculated and experimental $[\alpha]_D$ values range from 0.8 (for **19**) to 94.5 (for **16**). The average absolute deviation is 28.7; the RMS deviation is 37.0. For several molecules $[\alpha]_D$ values are small: for four molecules $[\alpha]_D < 30$. Given an average deviation of 28.7, one would expect calculated $[\alpha]_D$ values for some of these molecules to be of opposite sign compared to experimental $[\alpha]_D$ values. This is indeed the case: for (1*R*,5*R*)-*β*-pinene, **11**, the experimental and calculated $[\alpha]_D$ values are +23.1 and −26.1, respectively. For several molecules, deviations between calculated and experimental $[\alpha]_D$ values are >50: for **2**, **14**, **16**, **23**, **25**, and **26** the deviations are 53.1, 55.1, 94.5, 51.7, 51.1, and 73.6, respectively.

We have explored the sensitivity of predicted $[\alpha]_D$ values to the choice of equilibrium geometry and of the density functional and basis set used in calculating $[\alpha]_D$ for molecules **3**, **10**, and **11**, as detailed in Table 3. The variations are 82.2, 12.6, and 9.5, respectively. In no case is the sign of $[\alpha]_D$ changed.

For those molecules for which UV CD spectra have been reported we have carried out TDDFT calculations of electronic excitation energies, oscillator strengths, and rotational strengths, again using B3LYP/6-31G* geometries, the B3LYP functional, and the aug-cc-pVDZ basis set. The results are given in Tables 4−11 of the SI and compared to experimental UV absorption and ECD spectra in Figures 7−13 of the SI and in Figures 3−10. Simulated ECD spectra are obtained from calculated excitation energies and velocity rotational strengths, assuming Gaussian band shapes.[75]

In the case of *trans*-cyclooctene, **3** (Figure 3 and SI Table 4), ECD in cyclohexane was reported by Scott and Wrixon[7a] at wavelengths ≳185 nm and, subsequently, for gaseous **3** by Mason and Schnepp[53] at wavelengths ≳140 nm. Where overlapping, the solution and gas-phase spectra are quite similar. TDDFT calculations predict the first electronic excitation to be at 223 nm. Ten excitations lie between 180 and 223 nm; at $\lambda <$ 180 nm the density of excitations increases substantially. With the exception of excitations 4 and 8, whose ECD is predicted to be weakly positive, excitations 1−10 exhibit negative ECD, the strongest being for excitations 3, 5, 7, and 10. Excitations 11−30, lying in the range 180−150 nm, mostly exhibit positive ECD. To simulate the experimental ECD spectrum, we have used Gaussian band shapes. In Figure 3, the ECD spectrum of **3** is shown using two bandwidths, $\sigma = 0.2$ and 0.4 eV. Due to the high density of electronic excitations, the predicted ECD spectrum is quite sensitive to the choice of bandwidth; significantly less structure is apparent at 0.4 eV as compared to 0.2 eV. Comparison of calculated and experimental ECD spectra shows modest agreement. The negative ECD observed at 196 nm can be assigned to the negative ECD predicted at ∼215 nm, due predominantly to excitation 3. The positive ECD observed at 156.5 nm can be assigned to the positive ECD predicted at ∼170 nm. However, the strongly negative ECD predicted at 180−190 nm is not observed.

In the case of 2-bornene, **6** (Figure 4 and SI Table 5), ECD of gaseous **6** and of isooctane and 3-methylpentane solutions over the temperature range −182 to +60 °C was reported by Drake and Mason[7d] at wavelengths ≳185 nm. The solution and gas-phase spectra vary significantly; the peak of the predominantly negative CD is substantially red-shifted in solution relative to the gas phase. The first electronic excitation is predicted at 222 nm; six excitations lie between 190 and 222 nm. Excitations 1, 3, and 6 exhibit positive ECD; excitations 2, 4, and 5 exhibit negative ECD. As a result, positive ECD is predicted at 220−230 nm and negative ECD is predicted at ∼200 nm. Again, agreement of calculated and experimental spectra is modest: the negative ECD observed in the gas phase at 188 nm and in solution at ∼200 nm can be assigned to the predicted ECD at ∼200 nm. However, the positive ECD predicted at 220−230 nm is not observed in the experimental spectra.

In the case of α-pinene, **10** (Figure 5 and SI Table 6), ECD of gaseous **10** has been reported by Mason and Schnepp[53] and by Drake and Mason[7d] at wavelengths ≳140 and ≳175 nm, respectively. The spectra are qualitatively similar, where overlapping ECD of trifluoroethanol and 3-methylpentane solutions of **10** was also reported by Drake and Mason[7d] in the latter solvent at −95 and −182 °C. The ECD in cyclohexane solution was also reported by Scott and Wrixon[7a] at $\lambda \gtrsim 185$ nm. Again, solution and gas-phase spectra differ significantly. The first electronic excitation is predicted at 238 nm. Six excitations lie between 200 and 238 nm; at $\lambda <$ 200 nm the density of excitations increases substantially. Simulated ECD spectra exhibit multiple oscillations in sign, with negative, positive, and negative ECD at ∼240, 225, and 200 nm, respectively. Agreement with the experimental gas-phase spectrum is good, qualitatively, for the negative, positive, and negative features observed at ∼220, ∼200, and ∼185 nm. At lower wavelengths, agreement is poorer.

In the case of *β*-pinene, **11** (Figure 6 and SI Table 7), ECD spectra of gaseous **11** have been reported by Mason and Schnepp[53] and by Drake and Mason[7d] at wavelengths ≳140 and ≳165 nm, respectively. The spectra are qualitatively similar, where overlapping. ECD of 3-methylpentane solutions of **11** over the temperature range +20 to −100 °C was also reported by Drake and Mason.[7d] The ECD in cyclohexane solution was

(53) Mason, M. G.; Schnepp, O. *J. Chem. Phys.* **1973**, *59*, 1092−1098.

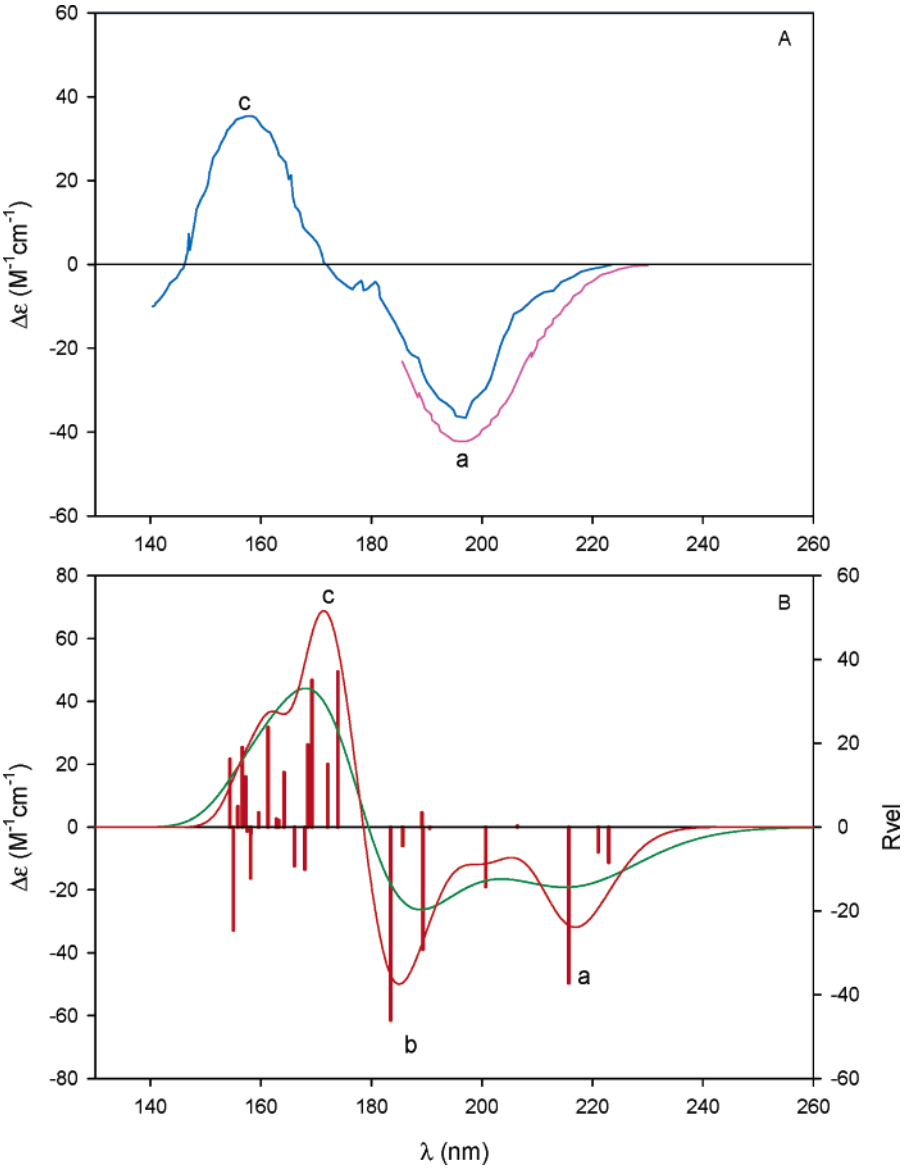

FIGURE 3. (A) Experimental ECD spectrum of (*R*)-(−)-*trans*-cyclooctene, **3**: (ref 53) (blue line) gas; (ref 7a) (pink line) in cyclohexane. (B) Velocity representation B3LYP/aug-cc-pVDZ//B3LYP/6-31G* rotational strengths and simulated ECD spectra: (red line) $\sigma = 0.2$ eV, (green line) $\sigma = 0.4$ eV.

also reported by Scott and Wrixon[7a] at $\lambda \gtrsim 185$ nm. In contrast to those of α-pinene, solution and gas-phase spectra are very similar. The first electronic excitation is predicted at 223 nm. Six excitations lie between 190 and 223 nm; at $\lambda < 190$ nm the density of excitations increases substantially. Simulated ECD spectra exhibit multiple oscillations in sign, with negative, positive, negative, and positive ECD at ∼215, ∼190, ∼170, and ∼160 nm, respectively. Agreement with the experimental spectra is good, qualitatively, the principal calculated features at 215, 190, and 160 nm corresponding to the observed ECD peaks at ∼200, ∼180, and ∼145 nm. The predicted negative ECD at ∼170 nm is not clearly observed.

In the case of camphene, **12** (Figure 7 and SI Table 8), ECD of gaseous **12** and of 3-methylpentane solutions over the temperature range +20 to −100 °C was reported by Drake and Mason.[7d] Significant differences between gas-phase and solution spectra were observed, and also significant variation with temperature was observed. TDDFT calculations predict the first electronic excitation to be at 218 nm. Five excitations lie between 190 and 218 nm. Only two, excitations 1 and 5, exhibit strong ECD, in both cases of negative sign. The predicted ECD spectrum is in modest agreement with the experimental gas-phase spectrum. The negative ECD predicted at ∼190 nm can be assigned to the negative experimental ECD at ∼200 nm. However, the negative ECD predicted at ∼220 nm is opposite in sign to that observed at this wavelength.

In the case of twistene, **14** (Figure 8 and SI Table 9), ECD of an isooctane solution has been reported by Drake and Mason[7d] at $\lambda \gtrsim 185$ nm. A single, positive feature was observed at ∼200 nm. The first electronic excitation is predicted at 227 nm. Six excitations lie between 190 and 227 nm. Four excitations, 1, 2, 5, and 6, exhibit strong ECD of positive, negative, positive, and negative signs, respectively. The observed ECD at 200 nm could be assigned either to excitation 1 or to excitation 5. Comparison of the predicted oscillator strengths to the experi-

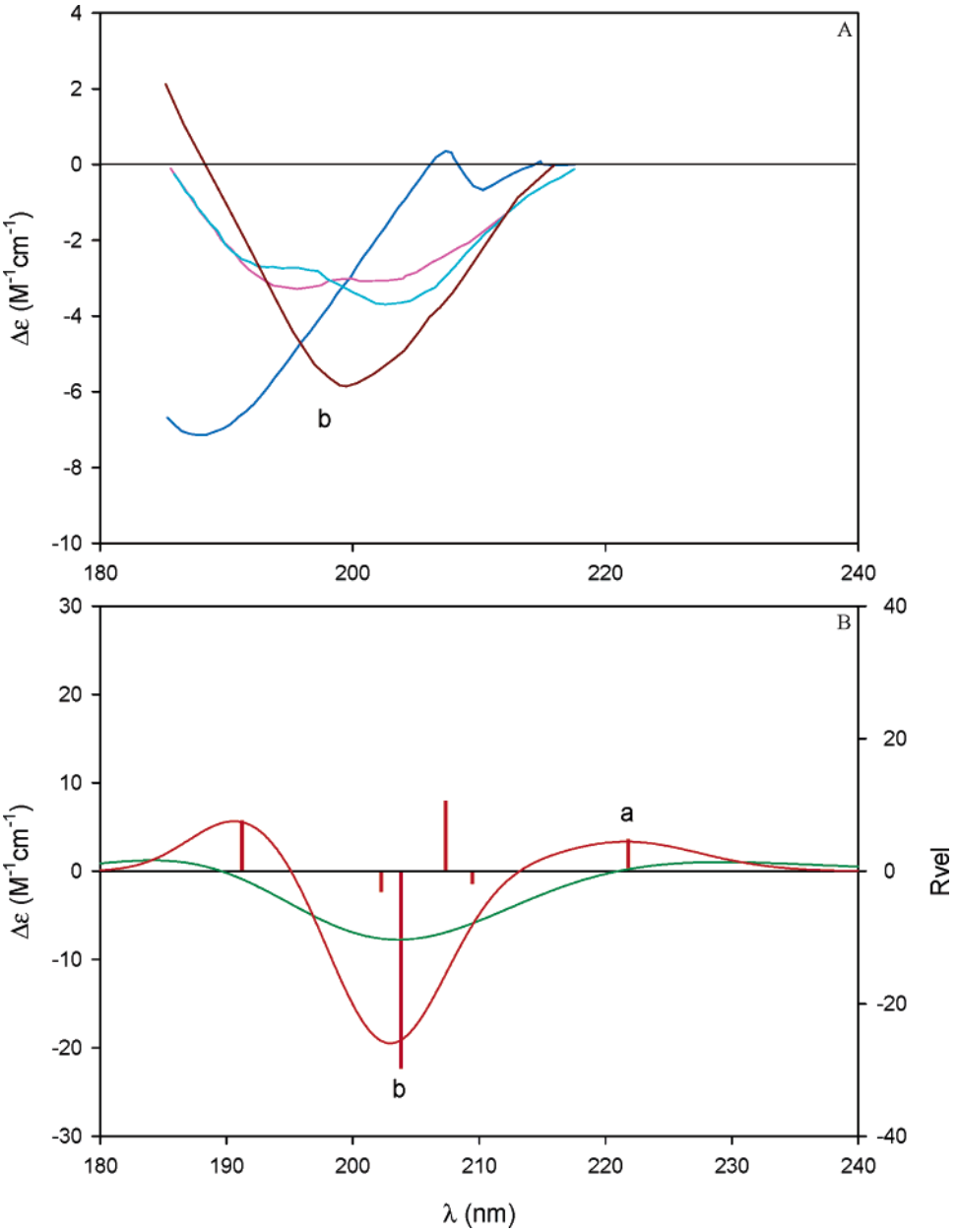

FIGURE 4. (A) Experimental ECD spectrum of (1*S*,4*R*)-(−)-2-bornene, **6**: (ref 7a) (blue line) gas, (pink line) in isooctane at 60 °C, (blue-green line) in isooctane at 20 °C, (brown line) in 3-methylpentane at −100 and −182 °C. (B) Velocity representation B3LYP/aug-cc-pVDZ//B3LYP/6-31G* rotational strengths and simulated ECD spectra: (red line) $\sigma = 0.2$ eV, (green line) $\sigma = 0.4$ eV.

mental absorption spectrum (SI Figure 12) suggests that the assignment to excitation 5 is more likely to be correct.

In the case of phyllocladene, **24** (Figure 9 and SI Table 10), ECD of a cyclohexane solution was reported by Scott and Wrixon[7a] at $\lambda \gtrsim 185$ nm. The first electronic excitation is predicted at 219 nm. Four excitations lie between 200 and 219 nm. At $\lambda < 200$ nm the density of excitations increases substantially. The predicted ECD spectrum exhibits a bisignate shape at $\lambda > 200$ nm, in agreement with the experimental spectrum.

In the case of *syn*-(*E*)-bisfenchylidene, **25** (Figure 10 and SI Table 11), ECD of an *n*-pentane solution was reported by Drake and Mason.[7d] The first excitation is predicted at 243 nm. Ten excitations lie between 200 and 243 nm. Of these, two, 6 and 10, exhibit strong ECD, in both cases negative. Ten excitations lie between 180 and 200 nm. Of these, two, 17 and 19, exhibit strong ECD, in both cases positive. The predicted ECD thus exhibits negative ECD at longer wavelengths and positive ECD at shorter wavelengths. Qualitatively, the predicted ECD is in agreement with the experimental ECD.

We have explored the sensitivity of predicted ECD spectra to the choice of the equilibrium geometry and of the density functional and basis set used in calculating electronic excitation energies and rotational strengths for molecules **3**, **10**, and **11**, with the results shown in Figures 14−22 of the SI. B3LYP/6-31G*, B3LYP/TZ2P, B3LYP/cc-pVTZ, HF/6-31G*, and MP2/6-31G* geometries have been used to examine the sensitivity to geometry. For all three molecules, very little variation in predicted ECD spectra is found over this range of geometries. The sensitivity to the functional is greater. For all three molecules ECD spectra predicted using the B3PW91 and PBE1PBE functionals are blue-shifted relative to the B3LYP

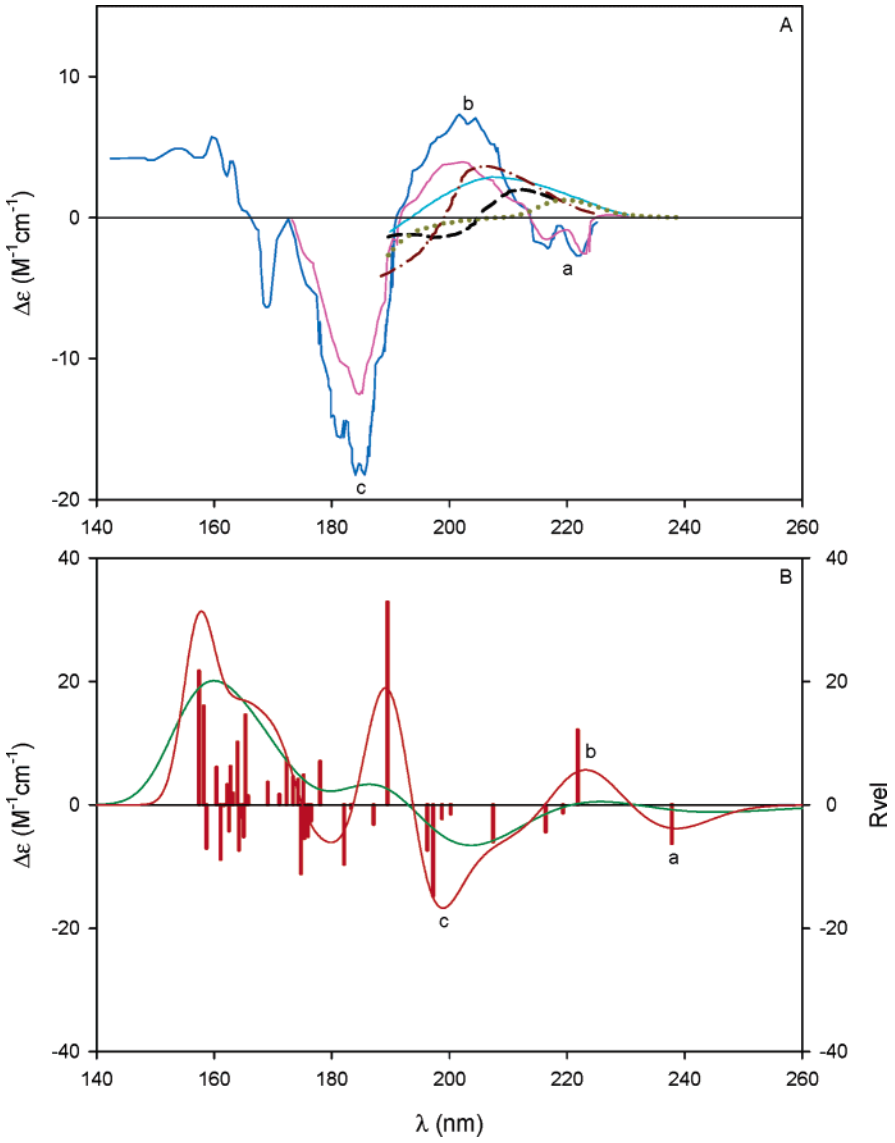

FIGURE 5. (A) Experimental ECD spectrum of (1*R*,5*R*)-(+)-α-pinene, **10**: (ref 53) (blue line) gas; (ref 7d) (pink line) gas, (blue-green line) in CF_3CH_2OH, (---) in 3-methylpentane at −95 °C, (-•-) in 3-methylpentane at −182 °C; (ref 7a) (•••) in cyclohexane. (B) Velocity representation B3LYP/aug-cc-pVDZ//B3LYP/6-31G* rotational strengths and simulated ECD spectra: (red line) $\sigma = 0.2$ eV, (green line) $\sigma = 0.4$ eV.

spectra. However, the shapes of the spectra are little changed. For all three molecules, the 6-311++G(2d,2p) basis set gives ECD spectra similar to the aug-cc-pVDZ spectra.

For molecules **9**, **10**, **11**, **14**, and **16** specific rotations have been reported at several visible−near-UV wavelengths. Experimental [α] values are compared to B3LYP/aug-cc-pVDZ//B3LYP/6-31G* values in Tables 12−16 of the SI. In Figure 11, we compare calculated and experimental [α] values for **9** and **16**. For **9**, the data reported in $CHCl_3$ by both Bellucci et al.[18] and Sadozai et al.[54] are in good agreement. Calculated [α] values are smaller than experimental values at all wavelengths, the difference increasing in magnitude with decreasing wavelength. For **16**, calculated [α] values are greater than the experimental values of Bellucci et al.,[18] the difference again increasing with decreasing wavelength. In Figure 12, we compare calculated and experimental [α] values for **10**. Experimental data were measured in these laboratories for solutions of **10** in seven diverse solvents during earlier studies of solvent effects on optical rotations.[2d] As seen in Figure 12, in a given solvent [α] increases smoothly with decreasing wavelength; the magnitude of the variation in [α] with solvent increases with decreasing wavelength. Gas-phase [α] values have also been reported at 355 and 633 nm by Vaccaro and co-workers[55] and lie within the range of values expected for the seven solvents (Figure 12). Calculated [α] values are smaller than all measured [α] values at all wavelengths. The difference between calculated and experimental [α] values increases with decreasing wavelength. In Figure 13, we compare calculated and experimental [α] values for **11**. Experimental data were measured in these laboratories for solutions of **11** in the same seven solvents as for **10**. As seen in Figure 13, all solutions give positive $[\alpha]_D$ values. As the wavelength decreases, [α] values increase to a maximum and then decrease. For some solvents [α] is negative

(54) Sadozai, S. K.; Lepoivre, J. A.; Dommisse, R. A.; Alderweireldt, F. C. *Bull. Soc. Chim. Belg.* **1980**, *89*, 637−642.

(55) Müller, T.; Wiberg, K. B.; Vaccaro, P. H.; Cheeseman, J. R.; Frisch, M. J. *J. Opt. Soc. Am. B* **2002**, *19*, 125−141. See ref 67a for a recent update of this work.

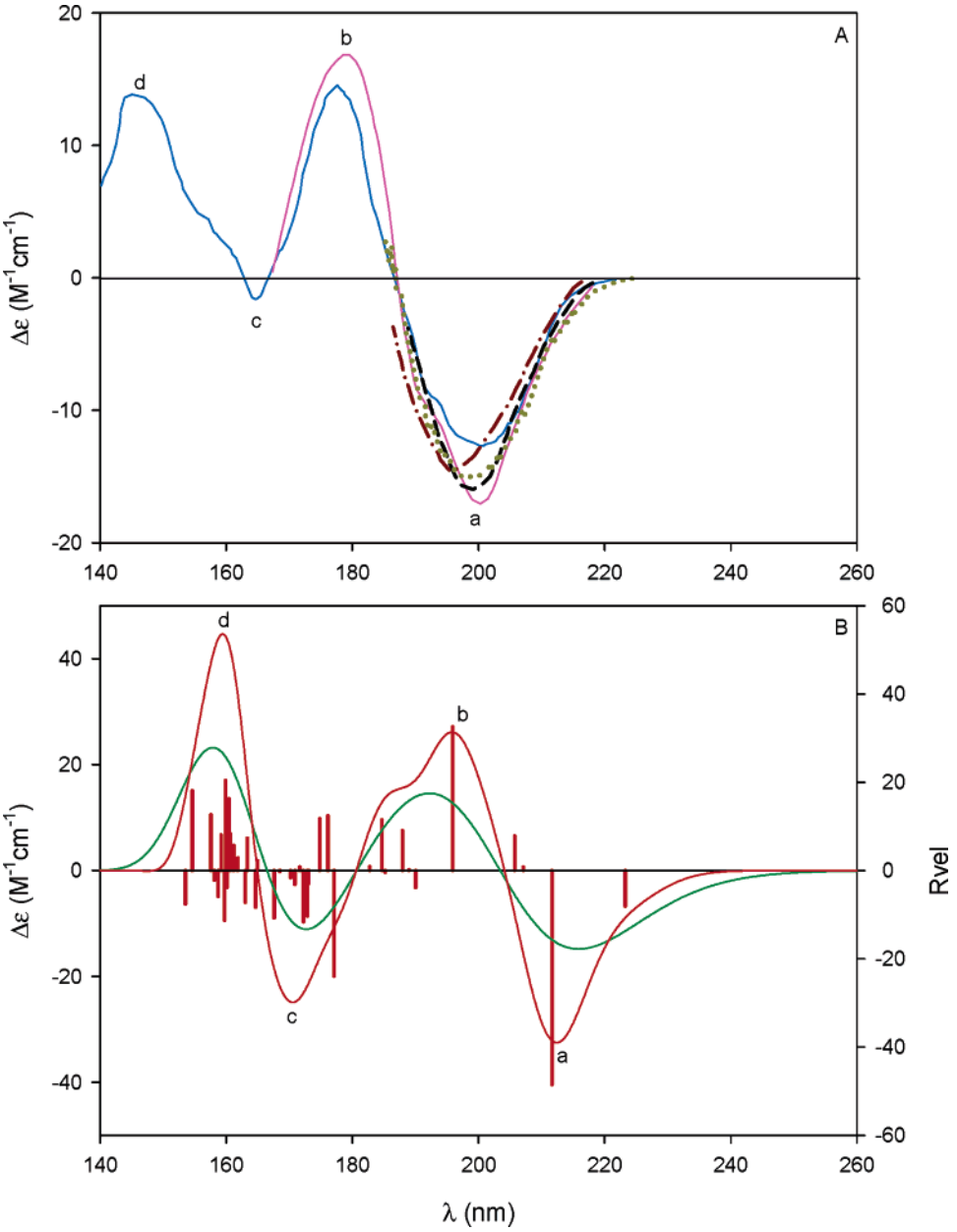

FIGURE 6. (A) Experimental ECD spectrum of (1*R*,5*R*)-(+)-*β*-pinene, **11**: (ref 53) (blue line) gas; (ref 7d) (pink line) gas, (---) in 3-methylpentane at 20 °C; (-·-) in 3-methylpentane at −100 °C; (ref 7a) (···) in cyclohexane. (B) Velocity representation B3LYP/aug-cc-pVDZ//B3LYP/6-31G* rotational strengths and simulated ECD spectra: (red line) $\sigma = 0.2$ eV, (green line) $\sigma = 0.4$ eV.

at 365 nm, while for others it is still positive. Our results are consistent with those of Müller et al. for cyclohexane solutions of **11**.[56] Gas-phase [α] values have also been reported at 355 and 633 nm (Figure 13).[55] At 633 nm [α] is small and positive; at 355 nm [α] is negative and considerably larger than any solution $[\alpha]_{365}$ value. Calculated [α] values are uniformly negative, increasing monotonically with decreasing wavelength. As far as the data extend, the difference between calculated and experimental [α] values increases with decreasing wavelength. In Figure 14, we compare calculated and experimental [α] values for **14**. Both calculated and experimental [α] values increase monotonically with decreasing wavelength. Quantitative agreement is excellent at all wavelengths.

We have also studied 3-*tert*-butylcyclohexene, **28** (Figure 15), synthesized by Belluci et al.[18] and Sadozai et al.[54] from *cis*- and *trans*-3-*tert*-butylcyclohexanols of known AC, respectively, whence the AC was assigned as *R*-(−)/*S*-(+). As with **9** and **16**, we have found two conformations, **a** and **b**. This conformational analysis is confirmed by a 2D scan of the potential energy surface of **28** as a function of the dihedral angles C1C6C5C4 and C1C2C3C4, shown in Figure 23 of the SI. Their structures are shown in Figure 4 of the SI; their ring dihedral angles are given in Table 2 of the SI. As detailed in Table 2, the B3LYP/6-31G* free energy difference of these conformations is <2 kcal/mol. Accordingly, at room temperature both conformations are expected to contribute to the specific rotation. On the basis of the relative free energies of **a** and **b**, their room temperature equilibrium populations are predicted to be 95%

(56) Müller, T.; Wiberg, K. B.; Vaccaro, P. H. *J. Phys. Chem. A* **2000**, *104*, 5959−5968.

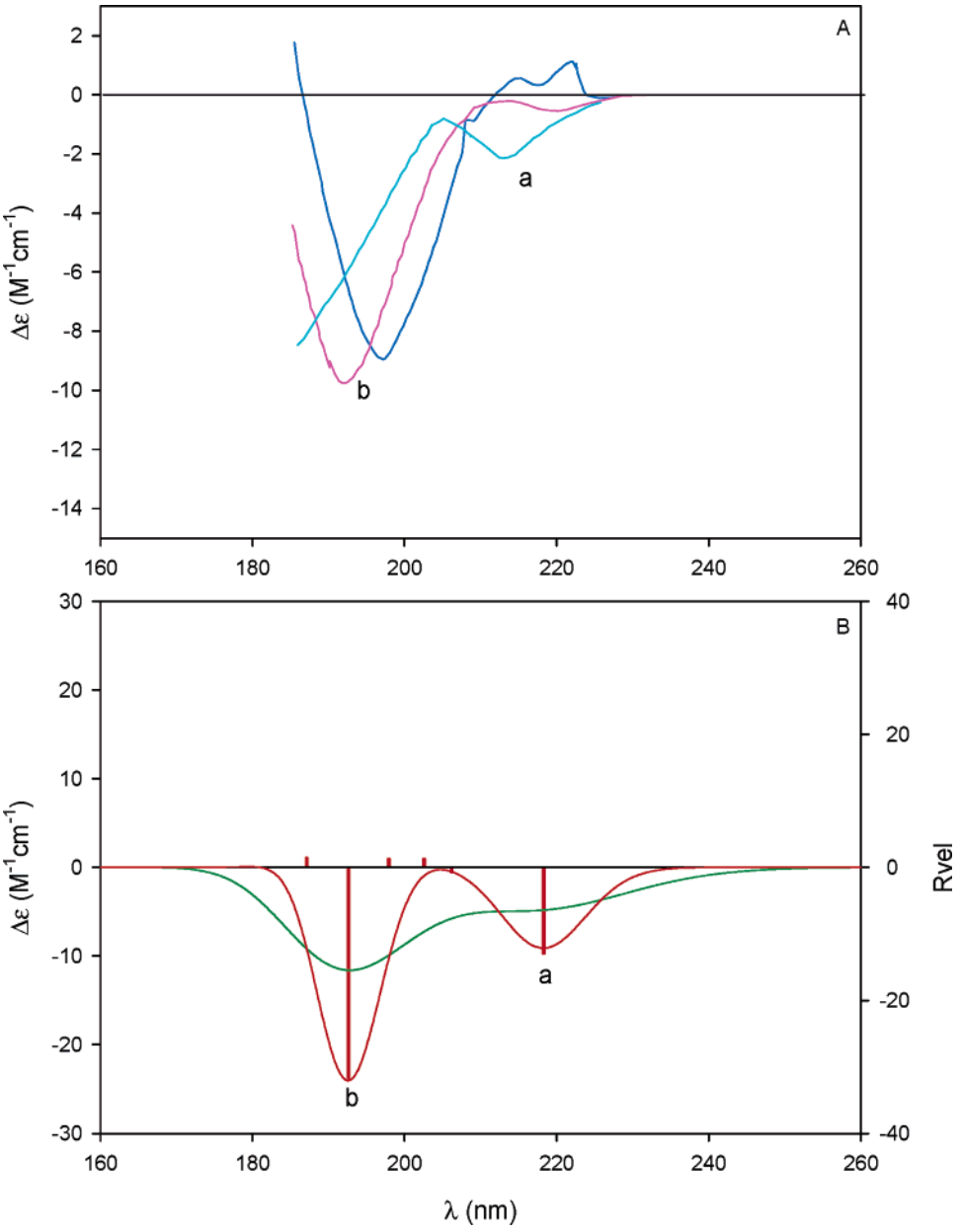

FIGURE 7. (A) Experimental ECD spectrum of (1*S*,4*R*)-(−)-camphene, **12**: (ref 7d) (blue line) gas, (pink line) in 3-methylpentane at 20 °C, (blue-green line) in 3-methylpentane at −100 °C. (B) Velocity representation B3LYP/aug-cc-pVDZ//B3LYP/6-31G* rotational strengths and simulated ECD spectra: (red line) $\sigma = 0.2$ eV, (green line) $\sigma = 0.4$ eV.

and 5%, respectively. Calculated [α] values at several wavelengths for conformations **a** and **b** of (3*R*)-**28** and for the room temperature equilibrium mixture of **a** and **b** are given in Table 4, together with the experimental values of Bellucci et al.[18] and Sadozai et al.[54] Conformationally averaged and experimental specific rotations are compared in Figure 11. Unlike the case of **9**, the two sets of experimental data are in poor agreement. While [α] values are negative for (3*R*)-**28** and increase in magnitude with decreasing wavelength for both data sets, at given wavelengths their magnitudes are substantially different. The difference most probably originates in differences in ee, the samples of Bellucci et al. being of markedly lower ee than those of Sadozai et al. In contrast to both sets of experimental data, calculated [α] values are positive, increasing in magnitude with decreasing frequency. The calculated $[\alpha]_D$ value differs from the Bellucci et al.[18] and Sadozai et al.[54] values by 71.4 and 158.4, respectively. The deviations increase with decreasing wavelength. Unlike β-pinene, **11**, the experimental [α] values do not change sign and agree in sign with experimental values at wavelengths <589 nm.

Finally, we have also studied the monoterpene *trans*-4-carene, **29** (Figure 15), obtained from naturally occurring 3-carene.[39] Its AC has been obtained by chemical correlation[41] and its $[\alpha]_D$ reported by Gollnick.[17] As with the *cis* isomer, **8**, Monte Carlo MMFF94 searching led to only one conformation. However, a B3LYP/6-31G* scan of the PES of **29** as a function of the dihedral angle C1C2C3C4 showed that two stable conformations exist, separated by a very low (∼2 kcal/mol) barrier (Figure 16). B3LYP/6-31G* optimization of the two conformations led to the structures shown in Figure 24 of the SI. In the lower energy conformation, **a**, the 3-methyl group is equatorial, while in the higher energy conformation, **b**, it is axial. The relative

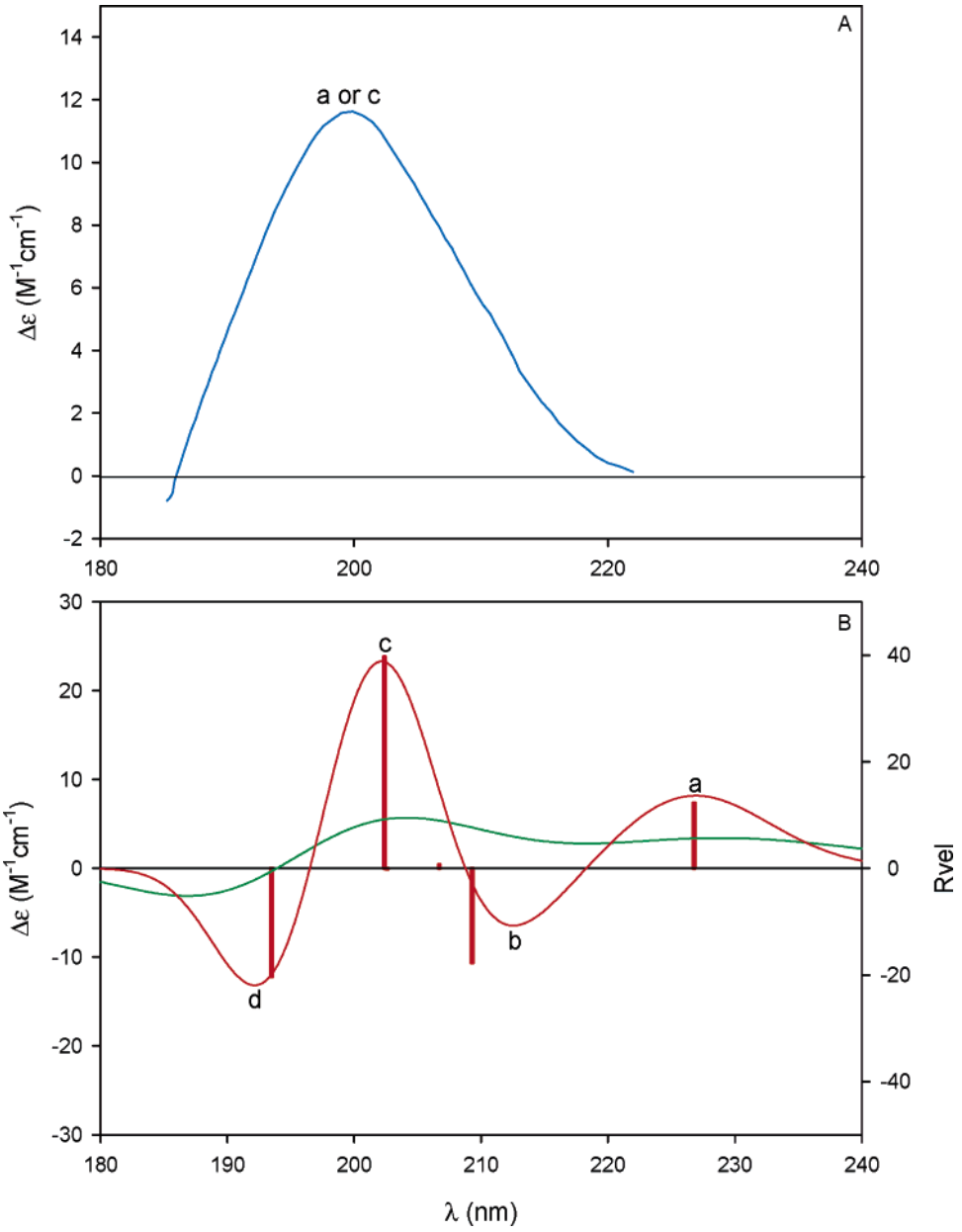

FIGURE 8. (A) Experimental ECD spectrum of (1*R*,4*R*,6*R*,9*R*)-(+)-twistene, **14**: (ref 7d) in isooctane. (B) Velocity representation B3LYP/aug-cc-pVDZ//B3LYP/6-31G* rotational strengths and simulated ECD spectra: (red line) $\sigma = 0.2$ eV, (green line) $\sigma = 0.4$ eV.

energies and free energies of **a** and **b** are 0.64 and 0.56 kcal/mol, respectively, leading to predicted room temperature equilibrium populations of 72% (**a**) and 28% (**b**). The calculated $[\alpha]_D$ values of **a** and **b** are −217.2 and −423.7, respectively; the conformationally averaged $[\alpha]_D$ is −275.3. The reported $[\alpha]_D$ in benzene is −167.48.[17]

Given the smallness of the barrier between conformations **a** and **b**, the assumption that **29** is limited to these two structures is likely to be inadequate. To estimate the contribution to $[\alpha]_D$ of the population of a range of structures of varying dihedral angle C1C2C3C4, we have calculated $[\alpha]_D$ as a function of C1C2C3C4 and obtained a Boltzmann-weighted average. The variation of $[\alpha]_D$ with C1C2C3C4 is shown in Figure 16 and detailed in Table 17 of the SI. Surprisingly, the average $[\alpha]_D$ resulting is −277.8, extremely close to the value obtained by averaging the $[\alpha]_D$ values of **a** and **b**. The calculated $[\alpha]_D$ of **29** thus remains >100 greater than the experimental value.

Discussion

Following the implementation of the TDDFT/GIAO methodology for the calculation of specific rotations,[2a,b] we reported B3LYP/aug-cc-pVDZ calculations of $[\alpha]_D$ values for 28 conformationally rigid chiral organic molecules of widely varying structure.[2c] For this set of molecules the average absolute deviation between calculated and experimental $[\alpha]_D$ values was 23.1; the maximum deviation was 70. Our subsequent study of 21 conformationally rigid chiral alkanes[6] found a very similar average absolute deviation, 24.8, the maximum deviation being 117. In this work, for a set of 26 conformationally rigid chiral alkenes, we have also found very similar results: the average absolute deviation is 27.4; the maximum deviation is 95. We therefore conclude that B3LYP/aug-cc-pVDZ//B3LYP/6-31G* $[\alpha]_D$ values for alkanes and alkenes are of comparable statistical accuracy.

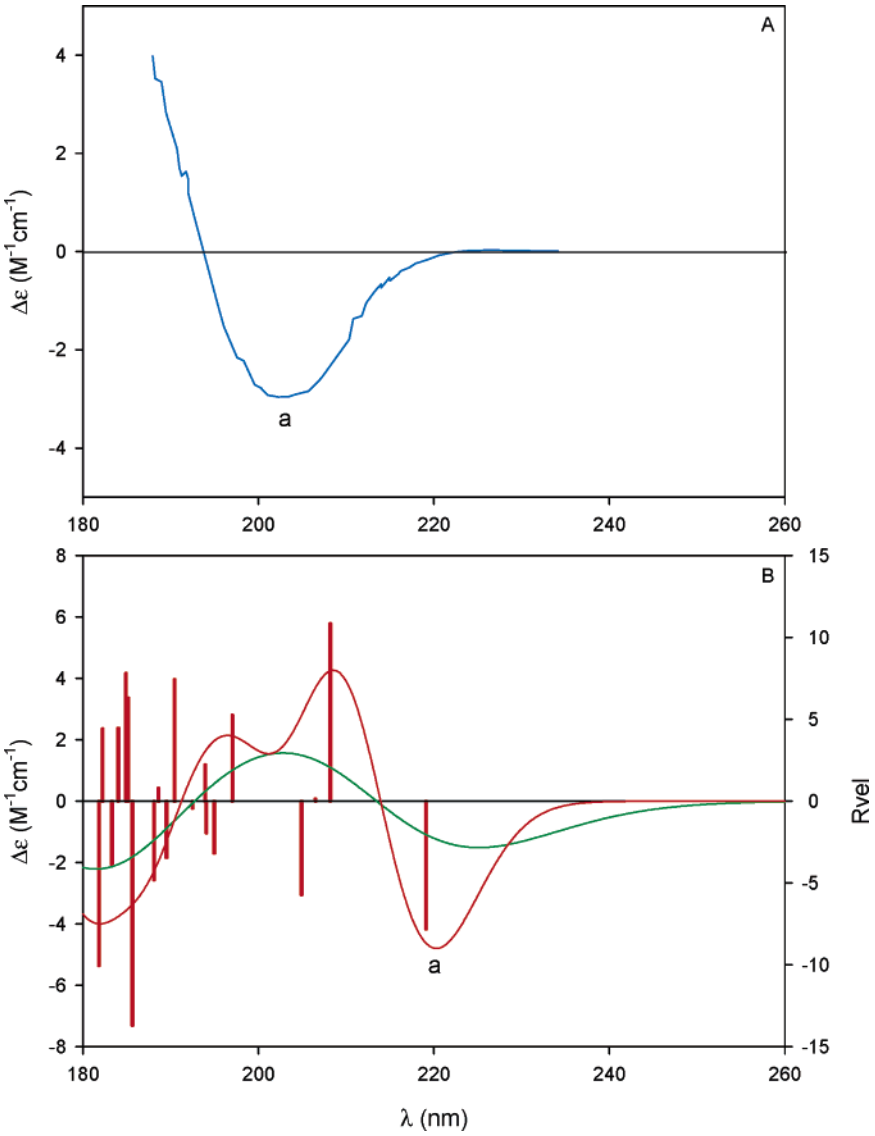

FIGURE 9. (A) Experimental ECD spectrum of (5*S*,8*S*,9*S*,10*S*,13*R*)-(+)-phyllocladene, **24**: (ref 7a) in cyclohexane. (B) Velocity representation B3LYP/aug-cc-pVDZ//B3LYP/6-31G* rotational strengths and simulated ECD spectra: (red line) $\sigma = 0.2$ eV, (green line) $\sigma = 0.4$ eV.

As we have discussed previously,[2c,4m] there are multiple possible origins of discrepancies between calculated and experimental $[\alpha]_D$ values. Experimental $[\alpha]_D$ values can be in error for a variety of reasons: (1) experimental error in the measurement of rotation; (2) chemical impurity of the sample; (3) concentration effects; (4) uncertainties in the ee. For compounds where multiple $[\alpha]_D$ values have been reported we have attempted to select the most reliable value. However, in many cases, information regarding chemical purity is limited and/or ee measurements were not reported. In no case was the concentration dependence of $[\alpha]_D$ reported, and the degree to which $[\alpha]_D$ values differ from the infinite dilution values is unknown. It is therefore likely that experimental errors in $[\alpha]_D$ values contribute significantly to the deviations between calculated and experimental $[\alpha]_D$ values. It should be noted, however, that the deviations cannot be *predominantly* attributed to errors in ee values: if incorrect, ee values would be uniformly <100%, $[\alpha]_D$ values correspondingly underestimated, and calculated $[\alpha]_D$ values systematically greater than experimental values, which is not the case (Figure 2).

Calculated $[\alpha]_D$ values can also be in error for many reasons: (1) incompleteness of the basis set; (2) inexactness of the density functional; (3) errors in the equilibrium geometries; (4) neglect of vibrational effects; (5) neglect of solvent effects. We have used the large basis set aug-cc-pVDZ containing diffuse functions, which we have previously shown to be essential for reducing basis set error to an acceptable level,[2a] in all calculations. Our prior study,[2c] in which B3LYP/aug-cc-pVDZ $[\alpha]_D$ values of 23 molecules were compared to values calculated using the much larger aug-cc-pVTZ basis set, found an average difference of only 7.9, demonstrating excellent convergence to the basis set limit of aug-cc-pVDZ $[\alpha]_D$ values. It is therefore very unlikely that basis set incompleteness contributes substantially to the deviation of calculated and experimental $[\alpha]_D$ values. The very small changes found for molecules **3**, **10**, and **11** when the 6-311++G(2d,2p) basis set is substituted for the aug-cc-pVDZ basis set (Table 3) are consistent with this conclusion.

The density functional we have used, B3LYP, is a state-of-the-art hybrid functional. In prior work, where alternative hybrid

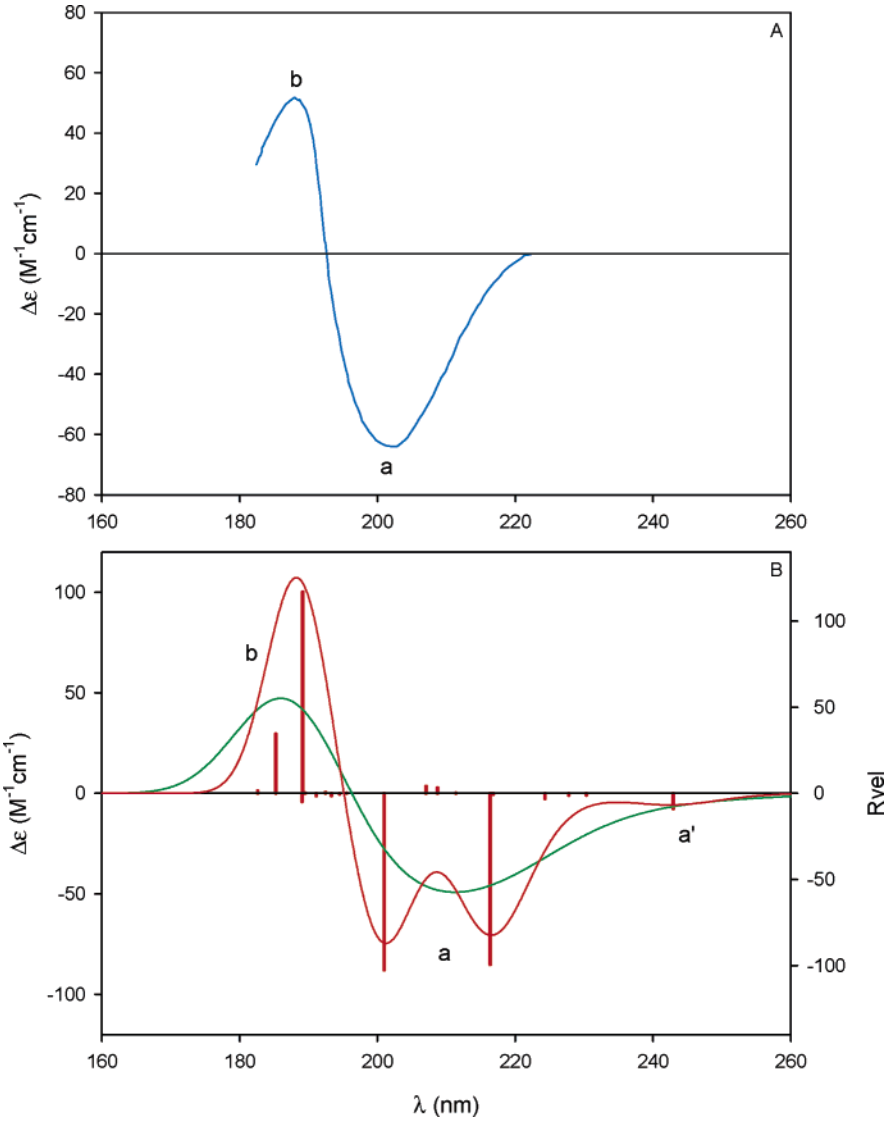

FIGURE 10. (A) Experimental ECD spectrum of (1*R*,4*S*,8*R*,11*S*)-(−)-*syn*-(*E*)-bisfenchylidene, **25**: (ref 7d) in *n*-pentane. (B) Velocity representation B3LYP/aug-cc-pVDZ//B3LYP/6-31G* rotational strengths and simulated ECD spectra: (red line) $\sigma = 0.2$ eV, (green line) $\sigma = 0.4$ eV.

functionals have been substituted for B3LYP, we have found small changes in $[\alpha]_D$ and no systematic improvement.[2a,b,4f] In this work, substitution of B3PW91 and PBE1PBE for B3LYP for molecules **3**, **10**, and **11** likewise gives very similar $[\alpha]_D$ values (Table 3). Accordingly, we expect that calculated $[\alpha]_D$ values for **1**−**26** are insensitive to the choice of hybrid functional. This does *not* mean, however, that errors in $[\alpha]_D$ values originating in inexactness of the functional are negligible. As we have discussed previously,[4g,h] the accuracy of the functional can be assessed by comparing calculated and experimental electronic excitation energies. We will return to this issue below when discussing ECD spectra.

We have used B3LYP/6-31G* equilibrium geometries in our calculations. Where studied, we have not previously observed large variations in $[\alpha]_D$ when other ab initio equilibrium geometries are used.[2a,b,4a,f] In this work, in the cases of molecules **10** and **11**, over a set of five geometries $[\alpha]_D$ variations are <10 (Table 3). However, in the case of **3**, over four geometries the range is 82. The much larger $[\alpha]_D$ obtained with the MP2/6-31G* geometry is surprisingly different from the B3LYP/6-31G*, B3LYP/TZ2P, and HF/6-31G* geometry values, given the very small differences in structural parameters for all four geometries (Table 1 of the SI). Greater sensitivity to the equilibrium geometry in other molecules than found in **10** and **11** cannot be excluded, and in some cases errors in B3LYP/6-31G* geometries could contribute significantly to the deviations of calculated and experimental $[\alpha]_D$ values.

The neglect of solvent effects in our calculations is undoubtedly a significant contributor to the deviation of calculated and experimental $[\alpha]_D$ values. In the cases of α- and *β*-pinene, **10** and **11**, we have previously reported the variation of $[\alpha]_D$ with solvent over a set of seven chemically diverse solvents,[2d] with the results shown in Figures 12 and 13 and Tables 13 and 14 of the SI. Solvent dependence of $[\alpha]_D$ has not been systematically studied for other molecules of the set **1**−**26**. In a few cases, $[\alpha]_D$ values have been reported for more than one solvent, but variations may originate in variations in chemical and enantiomeric purity as well as solvent effects. However, it is highly probable that solvent contributions to $[\alpha]_D$ are significant for all 26 molecules. Historically, following Condon,[57] chemists

(57) Condon, E. U. *Rev. Mod. Phys.* **1937**, *9*, 432−457.

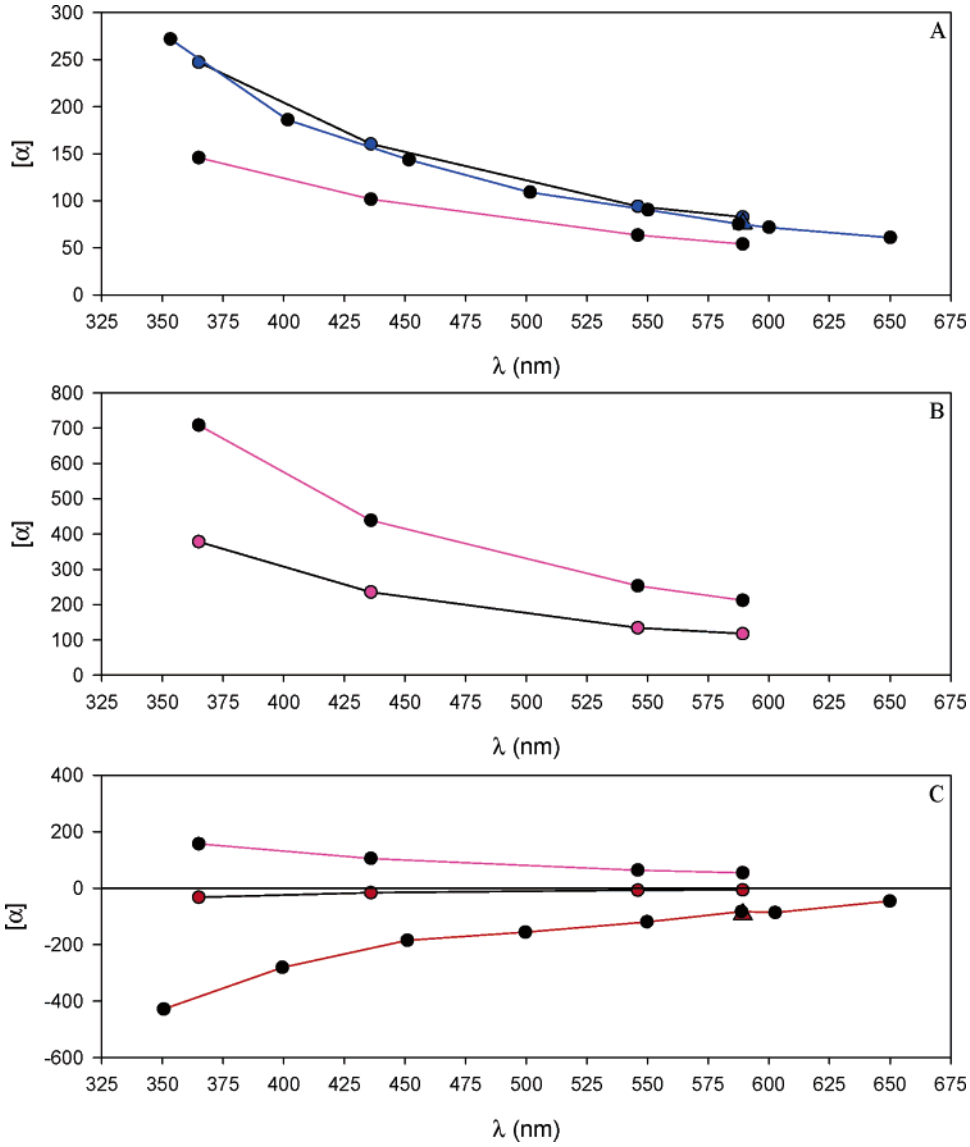

FIGURE 11. Calculated and experimental ORD of **9**, **16**, and **28**: (A) (4*R*)-(+)-**9**, ref 18 (blue circles), ref 54 (blue triangles) (black circles, blue line), calculated (black circles, pink line); (B) (3*R*,6*R*)-(+)-**16**, ref 18 (pink circles), calculated (black circles); (C) (3*R*)-(−)-**28**, ref 18 (red circles), ref 54 (red triangles) (black circles, red line), calculated (black circles, pink line). All calculations are with B3LYP/aug-cc-pVDZ//B3LYP/6-31G*. All experimental data are for $CHCl_3$ solutions.

have allowed for solvent effects on specific rotations by including the so-called Lorentz effective field correction factor, $(n^2 + 2)/3$ (where n is the solvent refractive index at the wavelength of the rotation measurement). We have previously examined the solvent dependence of the specific rotations of seven chemically diverse conformationally rigid molecules over a range of seven chemically diverse solvents and shown that changes in rotation with solvent exhibit little correlation with the function $(n^2 + 2)/3$.[2d] In addition, in our earlier study of 28 conformationally rigid molecules, we found that multiplying TDDFT/GIAO B3LYP/aug-cc-pVDZ//B3LYP/6-31G* $[\alpha]_D$ values by $(n^2 + 2)/3$ resulted in $[\alpha]_D$ values in statistically worse agreement with experiment.[2c] A much more sophisticated and reliable way to include the effects of a surrounding continuum dielectric on specific rotations is to use the polarizable continuum model (PCM). In prior work, the PCM was incorporated into the TDDFT/GIAO calculation of specific rotations and solvent effects calculated for seven molecules in seven solvents.[2d] The results were mixed: for some molecules and solvents predicted solvent effects were in good agreement with experiment; for others they were not. Notably, PCM calculations for the chlorinated solvents CCl_4 and $CHCl_3$ and the aromatic solvent C_6H_6 gave consistently poor results. We concluded that in some cases solvent effects are dominated by electrostatic solute−solvent interactions, while in other cases specific, covalent interactions are dominant. This conclusion has been supported by subsequent studies of solvent effects for several molecules by Vaccaro and co-workers.[67] To systematically include solvent effects in the prediction of specific rotations, a more sophisticated approach than the PCM is required. Hopefully, this will be developed soon.

The neglect of vibrational effects is also undoubtedly a significant contributor to the deviation of calculated and experimental $[\alpha]_D$ values. Direct proof of the existence of vibrational contributions to specific rotations has recently been provided by the demonstration of nonzero temperature depen-

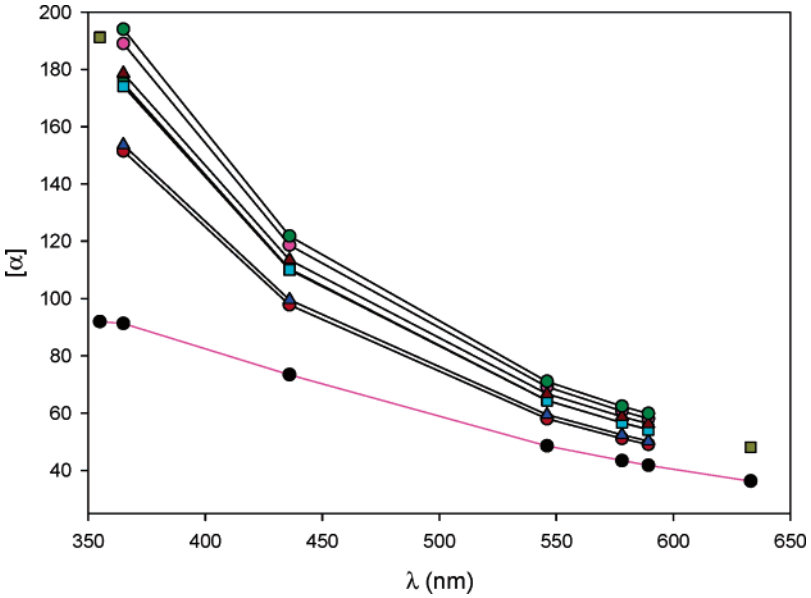

FIGURE 12. Calculated and experimental ORD of (1*R*,5*R*)-(+)-α-pinene, **10**: experimental, ref 2d and unpublished data, C_6H_{12} (red circles), CCl_4 (light green squares), C_6H_6 (blue triangles), $CHCl_3$ (pink circles), $(CH_3)_2CO$ (blue-green squares), CH_3OH (brown triangles), CH_3CN (dark green circles), ref 55, gas (tan squares); calculated, B3LYP/aug-cc-pVDZ//B3LYP/6-31G* (black circles).

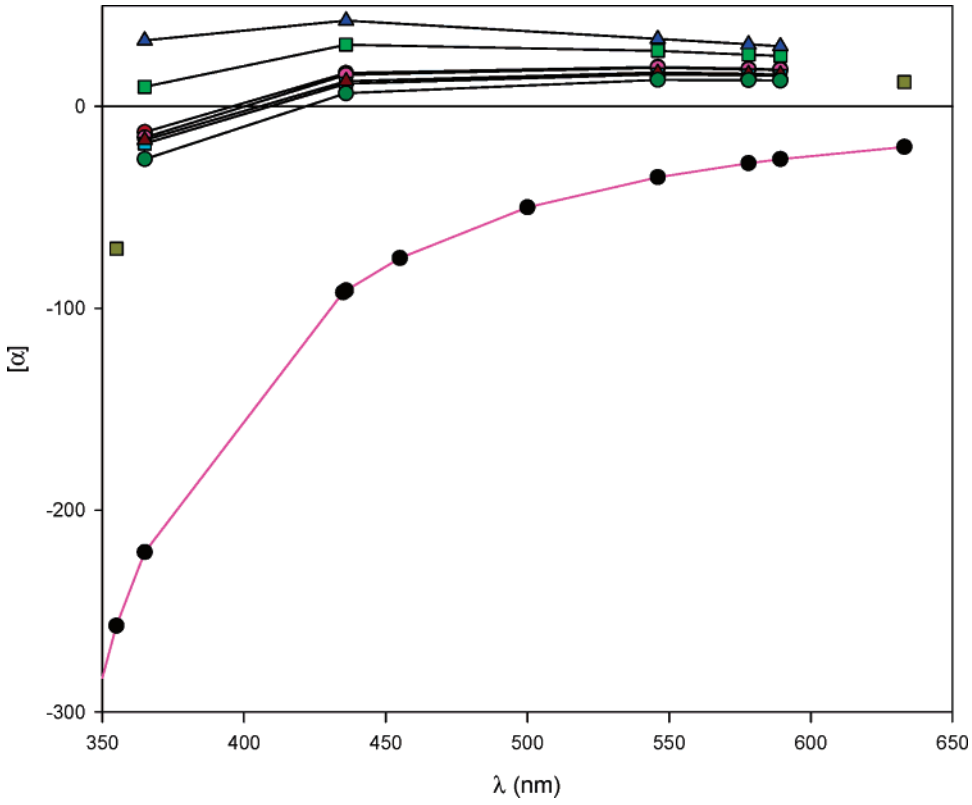

FIGURE 13. Experimental and calculated ORD of (1*R*,5*R*)-(+)-*β*-pinene, **11**: experimental, ref 2d and unpublished data, C_6H_{12} (red circles), CCl_4 (light green squares), C_6H_6 (blue triangles), $CHCl_3$ (pink circles), $(CH_3)_2CO$ (blue-green squares), CH_3OH (brown triangles), CH_3CN (dark green circles), ref 55, gas (tan squares); calculated, B3LYP/aug-cc-pVDZ//B3LYP/6-31G* (black circles).

dence of the specific rotations of several conformationally rigid molecules, including alkenes **10**−**12**, by Wiberg, Vaccaro, and co-workers.[58] To date, there have been very few attempts to predict vibrational contributions to specific rotations.[59,60] The most extensive study is that of Mort and Autschbach[60] in which DFT calculations were carried out for 22 molecules. Predicted vibrational contributions to $[\alpha]_D$ values were in the range 0.1−

(58) Wiberg, K. B.; Wang, Y.; Murphy, M. J.; Vaccaro, P. H. *J. Phys. Chem. A* **2004**, *108*, 5559−5563.

(59) (a) Ruud, K.; Taylor, P. R.; Astrand, P. O. *Chem. Phys. Lett.* **2001**, *337*, 217−223. (b) Ruud, K.; Zanasi, R. *Angew. Chem., Int. Ed.* **2005**, *44*, 3594−3596.

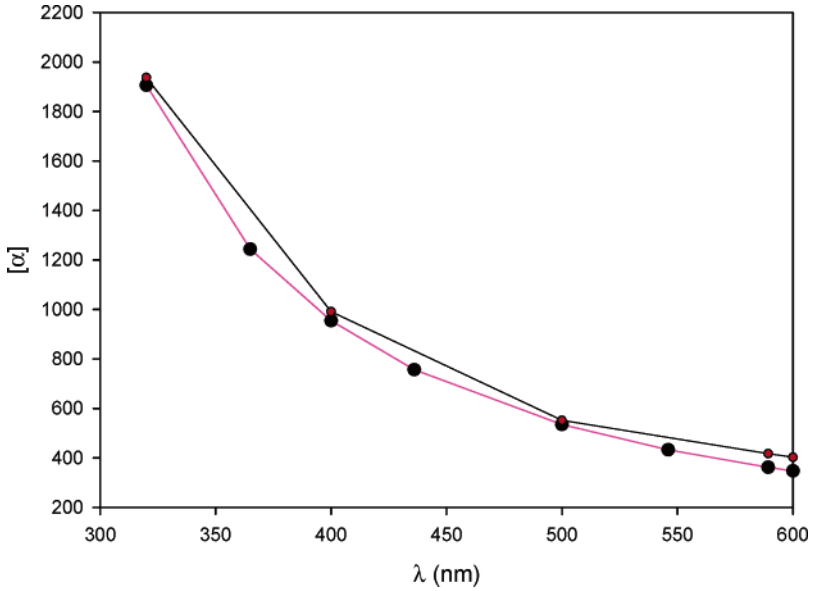

FIGURE 14. Comparison of experimental and calculated optical rotations at various wavelengths for (1*R*,4*R*,6*R*,9*R*)-(+)-twistene, **14**: experimental, ref 23, in EtOH solution (red circles); calculated, B3LYP/aug-cc-pVDZ//B3LYP/6-31G* (black circles).

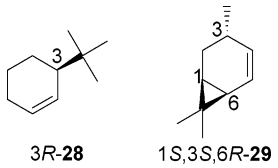

FIGURE 15. Molecules **28**, 3-*tert*-butylcyclohexene, and **29**, *trans*-4-carene.

TABLE 4. Calculated and Experimental [α] Values of (3*R*)-28[a]

	calcd[b]			exptl	
λ (nm)	**a**	**b**	av[c]	ref 18[d]	ref 54[e]
650					−46
603					−86
D	54.2	267.5	65.2	−6.2	−93.2
546	64.0	320.6	77.2	−7.4	−119
500					−156
451					−185
436	105.5	566.3	129.2	−16.1	
399					−281
365	157.5	938.0	197.7	−32.3	
351					−428

[a] $[\alpha]_D$ in deg $[dm \cdot g/cm^3]^{-1}$. [b] B3LYP/aug-cc-pVDZ//B3LYP/6-31G*. [c] Using B3LYP/6-31G* Δ*G* based populations at $T = 298$ K. [d] *c* 3.6, $CHCl_3$. [e] *c* 0.144, $CHCl_3$.

53.2. For the alkenes **1**, **2**, **3**, and **10** the values were +4.6, −18.2, −51.1, and +5.1, respectively. In some cases, including all four alkenes, inclusion of vibrational contributions reduced the differences between calculated and experimental $[\alpha]_D$ values. However, in other cases the opposite was found. The variable improvement in predicted $[\alpha]_D$ values may be due to (1) inadequacy of the algorithm used to calculate vibrational contributions (for example, the assumption that only cubic and quartic contributions to the force field need to be included), (2) neglect of the contributions of thermally populated excited vibrational states (the Mort−Autschbach calculations consider ground states only and cannot account for the temperature dependence of rotations), or (3) greater contributions of other sources of error in calculated and experimental rotations. Further studies of vibrational contributions, especially of their temperature dependence, are clearly necessary to establish a computational algorithm which can be routinely and reliably used to supplement vibration-independent TDDFT/GIAO calculations.

Despite the fact that calculated $[\alpha]_D$ values are not in perfect agreement with experimental values and the uncertainties in both calculated and experimental values, the results obtained for 26 alkenes of widely varying size, structure, and rigidity unquestionably demonstrate that the TDDFT/GIAO B3LYP/aug-cc-pVDZ//B3LYP/6-31G* methodology provides essentially reliable predictions of the $[\alpha]_D$ values of chiral alkenes. As a result, *with due recognition of the errors which do remain, we can conclude that* $[\alpha]_D$ *values predicted using this TDDFT methodology can constitute a useful basis for the assignment of the ACs of conformationally rigid chiral alkenes*.

The limits of the reliability of ACs assigned on the basis of TDDFT/GIAO calculations can be defined quantitatively on the basis of our results for the 26 alkenes **1**−**26**. The distribution of deviations between calculated and experimental $[\alpha]_D$ values, $[\alpha]_D$(calcd) − $[\alpha]_D$(exptl), using ACs for which $[\alpha]_D$(exptl) is positive, is plotted in Figure 17. For a large fraction, 13, of the 26 molecules, the absolute values of the deviations are <20, approximately equal numbers having positive and negative deviations. The number of molecules with absolute deviations >20 is smaller. Again, positive and negative deviations are almost equally numerous. Thus, as in our prior study of 65 molecules with experimental rotations ≤100,[4m] the deviations between calculated and experimental $[\alpha]_D$ values appear to be approximately random, exhibiting an approximately Gaussian distribution. The RMS deviation, σ, is 37.0. This enables the statistical reliability of future predictions of alkene $[\alpha]_D$ values for conformationally rigid molecules, and of ACs determined thence, to be defined.

Given a sample of a rigid chiral molecule whose AC is unknown, how do we assess the reliability of the AC obtained from the calculated $[\alpha]_D$? Let the experimental $[\alpha]_D$ value,

(60) Mort, B. C.; Autschbach, J. *J. Phys. Chem. A* **2005**, *109*, 8617−8623.

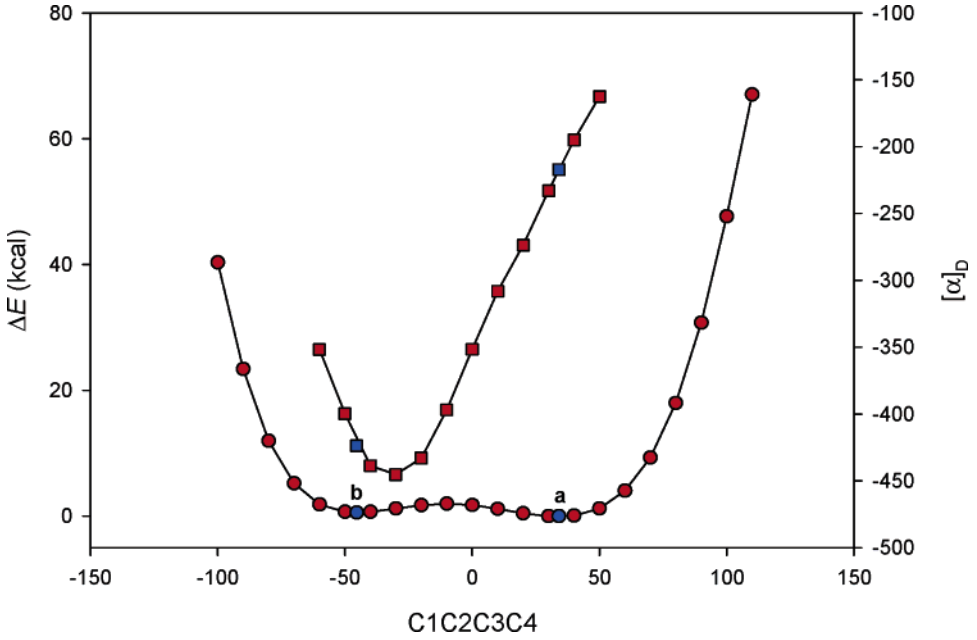

FIGURE 16. B3LYP/6-31G* PES scan and B3LYP/aug-cc-pVDZ $[\alpha]_D$ scan with respect to dihedral angle C1C2C3C4 for (1*S*,3*S*,6*R*)-**29**: energy (red circles), $[\alpha]_D$ (red squares). Optimized geometries: energy (blue circles), $[\alpha]_D$ (blue squares).

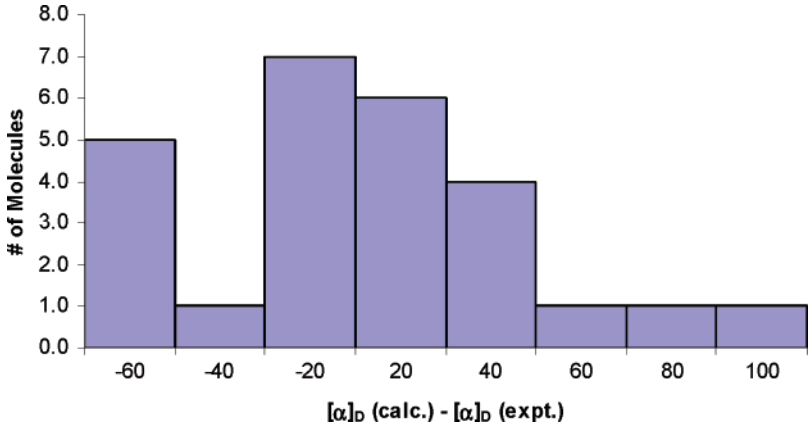

FIGURE 17. Distribution of deviations between calculated and experimental $[\alpha]_D$.

corrected to 100% ee, be $[\alpha]_D$(exptl) and the calculated values for the two enantiomers E_1 and E_2 be $[\alpha]_D(E_1)$ and $[\alpha]_D(E_2)$. We then calculate $[\alpha]_D(E_1) - [\alpha]_D(\text{exptl}) = \Delta(E_1)$ and $[\alpha]_D(E_2) - [\alpha]_D(\text{exptl}) = \Delta(E_2)$. If $|\Delta(E_1)| < 2\sigma = 74.0$ and $|\Delta(E_2)| > 74.0$, with 95% confidence we can assign the AC as E_1. If $|\Delta(E_1)| > 74.0$ and $|\Delta(E_2)| < 74.0$, the AC is E_2. If $|\Delta(E_1)|$ and $|\Delta(E_2)|$ are both < 74.0, the AC cannot be assigned with 95% confidence. Similarly, if both $|\Delta(E_1)|$ and $|\Delta(E_2)|$ are > 74.0, the AC is again indeterminate.

Let us apply these criteria to molecules **1**−**26**. In Figure 18, we compare calculated $[\alpha]_D$ values for both the correct AC and the opposite AC to the experimental $[\alpha]_D$ values using ACs for which $[\alpha]_D$(exptl) is positive. When the correct AC is used, all data points lie between the two lines of slope +1 with *y* axis intercepts of +74.0 and −74.0 except one, that for molecule **16**. When the incorrect AC is used, the same number of molecules lie between the two lines of slope −1 with intercepts +74.0 and −74.0. However, six molecules *also* lie between the two lines of slope +1. For these molecules, molecules **2**, **6**, **7**, **11**, **15**, and **24**, if the ACs were unknown, calculations of $[\alpha]_D$ would not be able to distinguish the two enantiomers. We refer to the area of the plot in Figure 18 lying simultaneously between the lines of slopes +1 and −1 as "the zone of indeterminacy".[4m] The ACs of molecules whose calculated and experimental $[\alpha]_D$ values place them in this zone cannot be determined with 95% confidence.

The above discussion assumes that an AC determined with 95% confidence is of acceptable reliability. One can of course adjust the error bar to be placed on calculated $[\alpha]_D$ values by adjusting the percent confidence level. Thus, if instead of 95% confidence one used 68% confidence, the error bars would change from $\pm 2\sigma$ to $\pm\sigma$. In our opinion ACs determined with significantly less than 90% confidence are essentially useless to organic chemists. After all, just guessing gives a result of 50% reliability. As a result, use of $\pm\sigma$ error bars would lower the confidence level to an unacceptable degree.

We turn now to the ECD spectra of molecules **3**, **6**, **10**, **11**, **12**, **14**, **24**, and **25**. The agreement between TDDFT B3LYP/aug-cc-pVDZ//B3LYP/6-31G* and experimental ECD spectra for these eight molecules is quite variable and ranges from

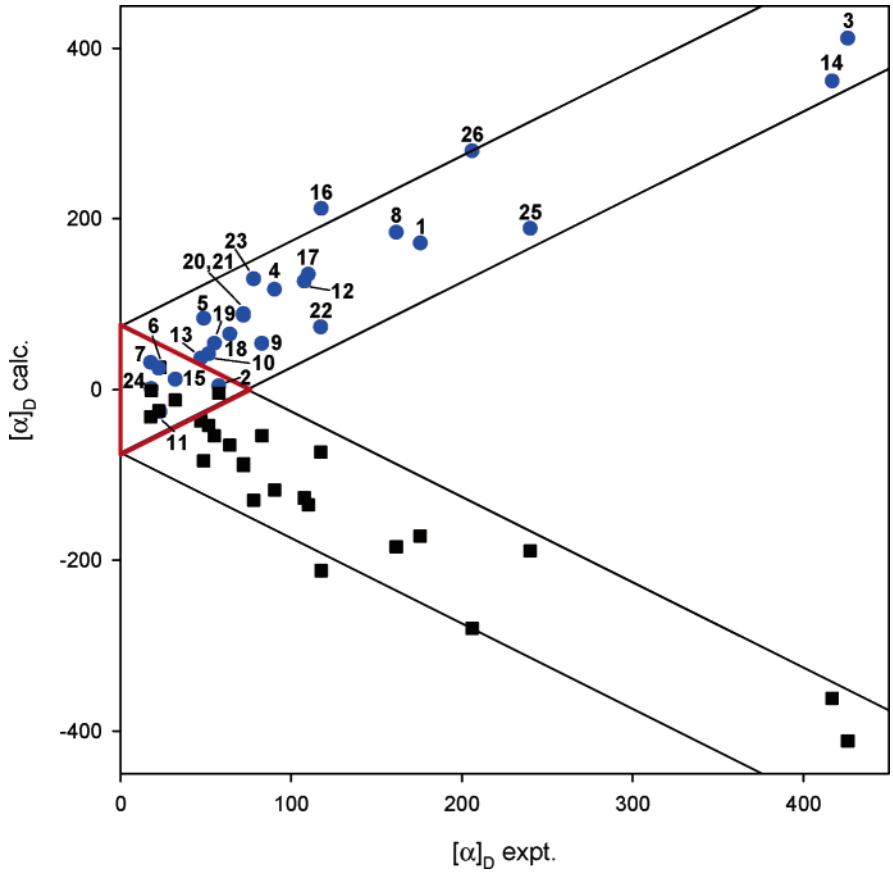

FIGURE 18. Comparison of experimental and calculated $[\alpha]_D$ for **1**−**26**: (blue circles) calculated with correct AC, (black squares) calculated with incorrect AC. The *y* axis intercepts are $+2\sigma$ and -2σ, where $2\sigma = 74.0$, and the lines have slopes $+1$ and -1. The triangle defined by the red lines is the "zone of indeterminacy".

modestly good to poor. In view of the complexity of the electronic spectrum of the simplest alkene, ethylene,[61] this is unsurprising. The lowest electronic excitations of the alkene chromophore are a mixture of valence and Rydberg excitations. Given the substantial widths of these excitations due to substantial differences between excited-state and ground-state potential energy surfaces, experimental spectra are a complex superposition of overlapping electronic transitions. In addition, the participation of Rydberg transitions results in significant sensitivity of the electronic spectrum to solvation. Of the molecules studied here, gas-phase and solution spectra have been compared for **3**, **6**, **10**, **11**, and **12**. In the cases of **6**, **10**, and **12**, substantial changes occur from gas-phase to solution spectra; in the cases of **3** and **11**, changes are minor. Our calculations are limited to vertical excitations at the ground-state equilibrium geometry and do not incorporate either vibronic effects or solvent effects. For comparison to experimental spectra Gaussian band shapes are assumed, a significant approximation. Differences between calculated and experimental ECD spectra can thus arise for various reasons: (1) errors in calculated excitation energies and rotational strengths; (2) neglect of vibronic effects; (3) differences between Gaussian and experimental band shapes; (4) in the case of spectra in solution, neglect of solvent effects in calculations.

Errors in calculated excitation energies and rotational strengths can originate in (1) basis set incompleteness, (2) inexactness of the density functional, and (3) error in the equilibrium geometry. The close agreement of rotational strengths calculated using the length and velocity representations (Tables 4−11, SI) demonstrates that basis set incompleteness is not a substantial cause of error. For molecules **3**, **10**, and **11** ECD spectra have been calculated using both aug-cc-pVDZ and 6-311++G(2d,2p) basis sets (Figures 16, 19, and 22 of the SI). The spectra change very little with a change in basis set, providing further support for the conclusion that basis set error is small. For these three molecules we have also examined the variation in the ECD spectrum with the choice of functional, comparing the B3LYP, B3PW91, and PBE1PBE functionals (Figures 15, 18, and 21 in the SI). Qualitatively, predicted spectra are very similar. Quantitatively, B3PW91 and PBE1PBE spectra are also very similar; however, B3LYP spectra are somewhat red-shifted, showing that the choice of functional is not insignificant. For **3**, **10**, and **11**, B3LYP ECD spectra are clearly red-shifted relative to the experimental spectra (Figures 3, 5, and 6) and the B3PW91 and PBE1PBE spectra are therefore in superior agreement with experiment. The variation in the ECD spectra of **3**, **10**, and **11** with the choice of equilibrium geometry (Figures 14, 17, and 20 of the SI) is small, and the use of the B3LYP/6-31G* geometry appears not to be a substantial source of error.

The neglect of vibronic contributions to calculated ECD spectra is likely to be a major source of error. Unfortunately, at this time the DFT calculation of excited-state potential energy

(61) See, for example, Wiberg, K. B.; de Oliveira, A. E.; Trucks, G. *J. Phys. Chem. A* **2002**, *106*, 4192−4199.

surfaces and of the vibrational profile of ECD spectra is impracticable.

The neglect of solvent effects on calculated ECD spectra is also undoubtedly a major source of error. The implementation of methods for including solvent effects, using the PCM within the GAUSSIAN program, is under way and, hopefully, will lead to more reliable predictions of solution ECD spectra.

On the basis of our results, we conclude that TDDFT B3LYP/aug-cc-pVDZ//B3LYP/6-31G* ECD calculations, neglecting vibronic and solvent effects, do not provide a straightforward, unambiguous basis for the assignment of the ACs of chiral alkenes. While in the best cases—e.g., β-pinene, **11**—the correspondence of calculated and experimental ECD spectra is certainly good enough to permit unambiguous assignment of the AC, in the worst cases—e.g., 2-bornene, **6**, and camphene, **12**—this is not so. In addition, in using ECD for the assignment of ACs it is obviously desirable that the experimental spectrum be measured at wavelengths <185 nm. This requires vacuum UV CD instrumentation, a considerable complication.

Our ECD calculations cast additional light on the results of our OR calculations. The specific rotation can be written as the sum of contributions of the electronic excitations:[4g]

$$[\alpha]_\lambda = \sum_i [\alpha]_\lambda^i \qquad [\alpha]_\lambda^i = \left(\frac{9147}{M}\right)\left(\frac{R_i \lambda_i^2}{(\lambda^2 - \lambda_i^2)}\right)$$

where λ_i and R_i are the wavelength and rotational strength of the ith excitation. Our calculations of electronic excitation energies and rotational strengths thus permit the contributions $[\alpha]_\lambda^i$ to $[\alpha]_\lambda$ to be calculated. For molecules **3**, **6**, **10**, **11**, **12**, **14**, **24**, and **25** these values are tabulated for all excitations calculated in Tables 4−11 of the SI. Inspection shows that, for every molecule, many excitations contribute significantly to $[\alpha]_D$, not just those of lowest energy. In the cases of **3**, **10**, and **11**, excitation energies, rotational strengths, and $[\alpha]_D^i$ values were calculated for large numbers of excitations (30, 40, and 40), up to excitation energies of ~8 eV. In each case, $[\alpha]_D^i$ values do not diminish systematically with increasing excitation energy. This will undoubtedly be the case with all other alkenes. It follows that one should not expect $[\alpha]_D$ to correlate with the ECD of the lowest excitations. For the molecules studied here, there is indeed very poor correlation. We note, for example, that the longest wavelength ECD of (+)-**11** and that of (+)-**24** are both negative.

Further evidence of the complex relationship between the OR and ECD phenomena is provided by our studies of the variations of predicted $[\alpha]_D$ values and ECD spectra with basis set, functional, and geometry. As discussed above, the predicted ECD spectra of **3**, **10**, and **11** are insensitive to variations in both basis set and equilibrium geometry. For **10** and **11**, this is also the case for predicted $[\alpha]_D$ values. However, for **3**, while $[\alpha]_D$ is basis set insensitive, a large increase occurs when the MP2/6-31G* geometry is used. Since the ECD spectrum to 165 nm is very little changed, it must be concluded that the excitations at λ < 165 nm contribute importantly to $[\alpha]_D$. Conversely, for **3**, **10**, and **11** we have found that the B3LYP ECD spectra change significantly on changing the functional to B3PW91 or PBE1PBE, while the changes in $[\alpha]_D$ are extremely small. Since B3LYP excitation energies for the lowest energy transitions are lower than for B3PW91 and PBE1PBE, one might expect that B3LYP $[\alpha]_D$ values would be greater. This is the case for **3** and **11**, but not for **10**. Thus, while perfect $[\alpha]_D$ values can only result when excitation energies and rotational strengths are perfectly predicted, at least for alkenes one cannot judge the reliability of $[\alpha]_D$ calculations by examining the comparison of calculated and experimental ECD spectra for only the lowest energy excitations.

While this work constitutes the first comprehensive study of the reliability of TDDFT calculations of $[\alpha]_D$ for chiral alkenes, TDDFT calculations for molecules **1**, **2**, **3**, **10**, and **11** have been previously reported. The results obtained using the largest basis sets employed are summarized in Table 5. In our earlier study of 28 conformationally rigid molecules, TDDFT/GIAO B3LYP/aug-cc-pVDZ and B3LYP/aug-cc-pVTZ $[\alpha]_D$ values were reported for **1**, **2**, and **10**.[2c] Simultaneously, Grimme reported TDDFT B3LYP calculations for **1**, **3**, **10**, and **11** using the SV(d)++ and aug-SV(d) basis sets.[2e] Since GIAOs were not used in these calculations, the rotations obtained were origin-dependent. Subsequently, Grimme reported origin-independent velocity representation TDDFT BP86/aug-cc-pVDZ calculations for **1** and **10**.[2f] Following these studies, Ziegler and co-workers reported TDDFT calculations for **1**−**3** and **10** using Slater orbital basis sets and pure functionals.[2g] GIAOs were not used, and the results were origin-dependent. Very recently, Mort and Autschbach[60] reported B3LYP/aug-cc-pVDZ TDDFT calculations for **1**−**3** and **10**, also without GIAOs. Overall, given the use of basis sets of sufficient size to minimize basis set errors, almost all calculations have given comparable results. The variations in $[\alpha]_D$ values can be attributed to variations in geometries, basis sets, and functionals (note that the B3LYP functional used by Grimme[2e,f] and Mort and Autschbach[60] is not identical to the B3LYP functional in the GAUSSIAN program) and, in some cases, the use of origin-dependent methods. Exceptions are the calculations for **3** by Ziegler and co-workers[2g] and by Mort and Autschbach[60] and the SAOP and SIC functional calculations for **2** and the SAOP calculations for **10** by Ziegler and co-workers.[2g] In the case of the calculations for **3**, the very large difference (nearly 100) between our $[\alpha]_D$ and that of Mort and Autschbach[60] led us to compare the structures used in these calculations. It has turned out that the Mort and Autschbach structure is that of the higher energy C_2-symmetry conformation **b** and not the lowest energy conformation **a** (see Table 1 of the SI).[62] Since the same structure was used by Ziegler and co-workers,[2g] the same explanation for their very different $[\alpha]_D$ values applies. With regard to the calculations on **2** and **10**, we attribute the significantly different $[\alpha]_D$ values, and greater deviations from experiment, to inadequacies of the SAOP and SIC functionals.

In Table 5 we also list the very small number of $[\alpha]_D$ values of alkenes obtained using the coupled-cluster (CC) methodology. Ruud et al. reported CC2 and CCSD $[\alpha]_D$ values for **1** and **2**.[63] Pederson and co-workers reported CC2 $[\alpha]_D$ values for **3**.[64] All of these calculations used the length representation for $[\alpha]_D$ and

(62) Professor J. Autschbach, private communication, 2006.

(63) Ruud, K.; Stephens, P. J.; Devlin, F. J.; Taylor, P. R.; Cheeseman, J. R.; Frisch, M. J. *Chem. Phys. Lett.* **2003**, *373*, 606−614.

(64) Pedersen, T. B.; Sanchez de Meras, A. M. J.; Koch, H. *J. Chem. Phys.* **2004**, *120*, 8887−8897.

(65) Pilati, T.; Simonetta, M. *J. Chem. Soc., Perkin Trans. 2* **1977**, 1435−1437.

(66) Brooks, P. R.; Bishop, R.; Counter, J. A.; Tiekink, E. R. T. *Z. Kristallogr.* **1993**, *208*, 319−321.

(67) (a) Wilson, S. M.; Wiberg, K. B.; Cheeseman, J. R.; Frisch, M. J.; Vaccaro, P. H. *J. Phys. Chem. A* **2005**, *109*, 11752−11764. (b) Wiberg, K. B.; Wang, Y.; Wilson, S. M.; Vaccaro, P. H.; Cheeseman, J. R. *J. Phys. Chem. A* **2005**, *109*, 3448−3453.

TABLE 5. Literature TDDFT Calculations of $[\alpha]_D$

molecule	ref	rep[a]	geometry	functional[b]	basis set	origin dependence[c]	$[\alpha]_D$(calcd)[d]	$[\alpha]_{calcd} - [\alpha]_{exptl}$[d]
(3*R*)-**1**	this work	L	B3LYP/6-31G*	B3LYP	aug-cc-pVDZ	O-I	171.6	−4.0
	2c	L	B3LYP/6-31G*	B3LYP	aug-cc-pVDZ	O-I	171.7	−3.9
		L	B3LYP/6-31G*	B3LYP	aug-cc-pVTZ	O-I	163.1	−12.5
	2e	L	B3LYP/SV(d)	B3LYP	SV(d)++	O-D	153.0	−22.6
		L	B3LYP/SV(d)	B3LYP	aug-SV(d)	O-D	153.2	−22.4
	2f	L	B3LYP/SV(P)	B3LYP	aug-cc-pVDZ	O-D	161.5	−14.1
		V	B3LYP/SV(P)	BP86	aug-cc-pVDZ	O-I	178.1	2.5
	2g	L	B3LYP/6-311G**	GGA	Vp	O-D	168.9	−6.7
		L	B3LYP/6-311G**	GGA	Vd	O-D	184.3	8.7
		L	B3LYP/6-311G**	SAOP	Vd	O-D	174.9	−0.7
		L	B3LYP/ 6-311G**	SIC	Vp	O-D	143.0	−32.6
	60	L	B3LYP/aug-cc-pVDZ	B3LYP	aug-cc-pVDZ	O-D	166.2	−9.4
	63	L	B3LYP/6-31G*	CC2	aug-cc-pVDZ	O-D	154.3	−21.3
		L	B3LYP/6-31G*	CCSD	aug-cc-pVDZ	O-D	128.9	−46.7
(2*S*,3*S*)-**2**	this work	L	B3LYP/6-31G*	B3LYP	aug-cc-pVDZ	O-I	−4.5	53.2
	2c	L	B3LYP/6-31G*	B3LYP	aug-cc-pVDZ	O-I	−3.4	54.2
		L	B3LYP/6-31G*	B3LYP	aug-cc-pVTZ	O-I	9.2	66.8
		L	B3LYP/6-311G**	GGA	Vp	O-D	12.2	69.8
		L	B3LYP/6-311G**	GGA	Vd	O-D	12.7	70.3
		L	B3LYP/6-311G**	SAOP	Vd	O-D	60.8	118.4
		L	B3LYP/6-311G**	SIC	Vp	O-D	43.9	101.5
	60	L	B3LYP/aug-cc-pVDZ	B3LYP	aug-cc-pVDZ	O-D	−11.7	45.9
	63	L	B3LYP/6-31G*	CC2	aug-cc-pVDZ	O-D	14.5	72.1
		L	B3LYP/6-31G*	CCSD	aug-cc-pVDZ	O-D	2.6	60.2
(*R*)-**3**	this work	L	B3LYP/6-31G*	B3LYP	aug-cc-pVDZ	O-I	−411.7	14.3
	2e	L	B3LYP/SV(d)	B3LYP	SV(d)++	O-D	−416.6	9.4
		L	B3LYP/SV(d)	B3LYP	aug-SV(d)	O-D	−417.0	9.0
	2g	L	B3LYP/6-311G**	GGA	Vp	O-D	−334.9	91.1
		L	B3LYP/6-311G**	GGA	Vd	O-D	−309.5	116.5
		L	B3LYP/6-311G**	SAOP	Vd	O-D	−280.7	145.3
		L	B3LYP/6-311G**	SIC	Vp	O-D	−294.2	131.8
	60	L	B3LYP/aug-cc-pVDZ	B3LYP	aug-cc-pVDZ	O-D	−322.7	103.4
	64	L	B3LYP/cc-pVTZ	CC2	aug-cc-pVDZ	O-D	−286.2	139.8
		L	B3LYP/cc-pVTZ	CC2	aug-cc-pVDT	O-D	−276.4	149.7
		L	B3LYP/cc-pVTZ	CC2	aug-cc-pVDQ	O-D	−272.1	153.9
(1*R*,5*R*)-**10**	this work	L	B3LYP/6-31G*	B3LYP	aug-cc-pVDZ	O-I	41.8	−9.8
	2c	L	B3LYP/6-31G*	B3LYP	aug-cc-pVDZ	O-I	41.9	−9.7
		L	B3LYP/6-31G*	B3LYP	aug-cc-pVTZ	O-I	41.4	−10.2
	2e	L	B3LYP/SV(d)	B3LYP	SV(d)++	O-D	44.2	−7.4
		L	B3LYP/SV(d)	B3LYP	aug-SV(d)	O-D	47.8	−3.8
	2f	L	B3LYP/SV(P)	B3LYP	aug-cc-pVDZ	O-D	42.0	−9.6
		V	B3LYP/SV(P)	BP86	aug-cc-pVDZ	O-I	37.7	−13.9
	2g	L	B3LYP/6-311G**	GGA	Vp	O-D	45.1	−6.5
		L	B3LYP/6-311G**	GGA	Vd	O-D	59.3	7.7
		L	B3LYP/6-311G**	SAOP	Vd	O-D	83.4	31.8
		L	B3LYP/6-311G**	SIC	Vp	O-D	63.0	11.4
	60	L	B3LYP/aug-cc-pVDZ	B3LYP	aug-cc-pVDZ	O-D	41.2	−10.5
(1*R*,5*R*)-**11**	this work	L	B3LYP/6-31G*	B3LYP	aug-cc-pVDZ	O-I	−26.1	−49.2
	2e[e]	L	B3LYP/SV(d)	B3LYP	SV(d)++	O-D	−55.2	−78.3
		L	B3LYP/SV(d)	B3LYP	aug-SV(d)	O-D	−21.3	−44.4

[a] L = length representation. V = velocity representation. [b] Note that the B3LYP functional used in refs 2e−g and 60 is *different* from the B3LYP functional used in the GAUSSIAN program and in ref 2c. [c] O-I = origin-independent. O-D = origin-dependent. [d] $[\alpha]_D$ in deg $[dm \cdot g/cm^3]^{-1}$. [e] The incorrect AC used for **11** has been corrected.

gave origin-dependent results. All CC $[\alpha]_D$ values are in poorer agreement with experiment than the TDDFT/GIAO B3LYP/aug-cc-pVDZ//B3LYP/6-31G* values. The difference is dramatically greater for **3**: for all three large basis sets, aug-cc-pVXZ (X = D, T, and Q), the differences from the experimental $[\alpha]_D$ value are >100 larger than for TDDFT/GIAO calculations.[64] We have confirmed that the structure used for the CC calculations is indeed the lowest energy conformation. The difference thus reflects the difference in method, not geometry. Another molecule where CC $[\alpha]_D$ calculations were enormously less accurate than TDDFT/GIAO $[\alpha]_D$ calculations is norbornenone.[63] Alkene **3** increases the number of molecules for which CC calculations have so far provided much poorer accuracy than TDDFT/GIAO calculations.

In contrast, very few TDDFT calculations of ECD spectra have previously been reported for chiral alkenes. Grimme and Waletzke[71] and Diedrich and Grimme[72] have reported TDDFT calculations for **3**, using the BHLYP functional, and for **10**, using the BHLYP, B3LYP, and BP86 functionals, respectively. While the geometries and basis sets used differ from those used in this work, the B3LYP excitation energies, rotational strengths, and ECD spectrum of **10** are very nearly identical to our results. In contrast, the BHLYP ECD spectrum of **3** is qualitatively very different from our B3LYP, B3PW91, and PBE1PBE ECD

spectra. Only negative ECD is predicted for (*R*)-**3**, in major disagreement with the bisignate experimental ECD. While the geometry and basis set used differ from those used in our work, we attribute the difference in predicted ECD spectra to the lower accuracy of the BHLYP functional. This functional gives much less accurate predictions for electronic ground-state properties,[73] and this is likely to be the case for excited-state properties.

In addition to TDDFT calculations, CC calculations have been reported for **3** and **10** by Pedersen and Koch[74] and by Diedrich and Grimme,[72] respectively. In Figure 25 of the SI, the CCSD/aug-cc-pVDZ calculations of the ECD spectrum of **3** for the lowest 10 excitations are compared to those of the experimental spectrum. The CCSD spectrum is qualitatively similar to our B3LYP/aug-cc-pVDZ spectrum of the lowest 10 excitations. The CCSD excitation energies are however substantially higher. In contrast to our B3LYP spectrum, where the lowest energy band is predicted at lower energy than the experimental band, CCSD predicts the lowest energy band at higher energy than observed. Since the CCSD calculations are limited to only 10 excitations, it is unknown whether the experimental positive ECD at ∼160 nm would be successfully reproduced, as is the case for our TDDFT calculations. The CC2 ECD spectrum of **10** is qualitatively similar to the TDDFT/B3LYP spectrum at lower energies, but completely different at higher energies. In the latter region, no calculations are in agreement with experiment. As for **3**, CC2 excitation energies are substantially higher than for TDDFT/B3LYP. These results suggest that the much lower $[\alpha]_D$ for **3** predicted by CC2,[64] as compared to the experimental value, is at least in part caused by the systematic overestimation of electronic excitation energies by this methodology. A similar conclusion was previously arrived at for norbornenone.[63]

The 26 alkenes **1**−**26** have been classified as conformationally rigid on the basis of conformational analyses at the B3LYP/6-31G* level. For a number of molecules, specifically **1**, **2**, **4**−**8**, **10**−**14**, **18**, **19**, **21**, **25**, and **26**, we have found only one stable conformation. For others, **3**, **9**, **15**−**17**, **20**, and **22**−**24**, multiple stable conformations have been identified. In all of the latter cases, the second-to-lowest free energy conformation is >2.5 kcal/mol higher than the lowest free energy conformation, leading to the conclusion that only the latter is significantly populated at room temperature. We recognize, of course, that substantial errors in our predicted relative free energies leading to overestimation of the free energies of excited conformations would render this conclusion incorrect, leading in turn to contributions to $[\alpha]_D$ from excited conformations and to errors in $[\alpha]_D$ values predicted assuming conformational rigidity. Errors in conformational populations thus in principle could also contribute in some cases to errors in our calculated $[\alpha]_D$ values.

While studying the cyclohexenes **9** and **16**, we have also studied the 3-*tert*-butyl isomer of **9**, **28**. As with **9** and **16**, two conformations were found, with oppositely puckered cyclohexene rings. However, in contrast to **9** and **16**, the free energy difference of conformations **a** and **b** was predicted to be <2 kcal/mol, leading to a predicted room temperature population of 5% for conformation **b**. Calculated $[\alpha]_D$ values for conformations **a** and **b** of (3*R*)-**28** are 54.2 and 267.5, respectively, showing that significant population of **b** can significantly change the predicted $[\alpha]_D$. Calculations at four wavelengths from 589 to 365 nm predict that $[\alpha]$ values of **a** and **b** increase monotonically with decreasing wavelength, that at all wavelengths $[\alpha]$ values of **a** and **b** are of the same sign, and that the conformationally averaged $[\alpha]$ values are uniformly greater than the values of **a**, the difference increasing with decreasing wavelength. Very surprisingly, given the results obtained for **9** and **16**, predicted $[\alpha]$ values for **28** are uniformly opposite in sign to the experimental values. This error could originate in (1) errors in calculated $[\alpha]$ values of **a** and **b**, (2) error in the experimental $[\alpha]$ values, and (3) error in the assigned AC of **28**. Note that error in the predicted equilibrium populations of **a** and **b** cannot be the source, since the predicted sign of $[\alpha]$ at all wavelengths is independent of the value of the free energy difference. It seems most likely that it is the TDDFT calculations which are in error. At the sodium D line, calculated and experimental $[\alpha]$ values differ by 71.4 and 158.4 for the Bellucci et al. and Sadozai et al. experimental $[\alpha]_D$ values. The former error is within the range observed for **1**−**26**; the latter is considerably larger. Thus, if the data of Bellucci et al. are correct, the error is not unanticipated; if the data of Sadozai et al. are correct, the error is surprisingly large. Given the large difference in the two sets of experimental $[\alpha]$ values, the possibility that neither is correct cannot be totally excluded. A redetermination of the experimental ORD of **28** would be of value in assessing this possibility. Last, it would be worthwhile to reconfirm the AC of **28**, for example, by VCD spectroscopy, which is currently the most reliable chiroptical methodology for determining ACs.[68]

If it turns out that it is indeed the TDDFT calculations which are the principal source of error in predicting the sign of the ORD of **28**, it should be noted that the case of **28** differs qualitatively from that of β-pinene, **11**, the one molecule in the set **1**−**26** for which the sign of $[\alpha]_D$ is also incorrectly predicted. In the case of **11**, while the predicted $[\alpha]_D$ is of the wrong sign, at shorter wavelengths, predicted and experimental $[\alpha]$ values become cosignate, due to the change in sign of the experimental $[\alpha]$ values. This is not the case for **28**. Thus, **28** provides another example of a molecule where calculated and experimental $[\alpha]$ values increase monotonically with decreasing wavelength but are of the opposite sign at all wavelengths throughout the

(68) (a) Stephens, P. J. *J. Phys. Chem.* **1985**, *89*, 748−752. (b) Stephens, P. J.; Lowe, M. A. *Annu. Rev. Phys. Chem.* **1985**, *36*, 213−241. (c) Stephens, P. J. *J. Phys. Chem.* **1987**, *91*, 1712−1715. (d) Stephens, P. J. The Theory of Vibrational Circular Dichroism. *Encyclopedia of Spectroscopy and Spectrometry*, Academic Press: London, 2000; pp 2415−2421. (e) Ashvar, C. S.; Stephens, P. J.; Eggimann, T.; Wieser, H. *Tetrahedron: Asymmetry* **1998**, *9*, 1107−1110. (f) Aamouche, A.; Devlin, F. J.; Stephens, P. J. *Chem. Commun.* **1999**, *4*, 361−362. (g) Stephens, P. J.; Devlin, F. J. *Chirality* **2000**, *12*, 172−179. (h) Aamouche, A.; Devlin, F. J.; Stephens, P. J. *J. Am. Chem. Soc.* **2000**, *122*, 2346−2354. (i) Aamouche, A.; Devlin, F. J.; Stephens, P. J.; Drabowics, J.; Bujnicki, B.; Mikolajczyk, M. *Chem.*−*Eur. J.* **2000**, *6*, 4479−4486. (j) Stephens, P. J.; Aamouche, A.; Devlin, F. J.; Superchi, S.; Donnoli, M. I.; Rosini, C. *J. Org. Chem.* **2001**, *66*, 3671−3677. (k) Devlin, F. J.; Stephens, P. J.; Scafato, P.; Superchi, S.; Rosini, C. *Tetrahedron: Asymmetry* **2001**, *12*, 1551−1558. (l) Stephens, P. J.; Devlin, F. J.; Aamouche, A. In *Chirality: Physical Chemistry*; Hicks, J. M., Ed.; ACS Symposium Series; American Chemical Society: Washington, DC, 2002; Vol. 810, Chapter 2, pp 18−33. (m) Devlin, F. J.; Stephens, P. J.; Scafato, P.; Superchi, S.; Rosini, C. *Chirality* **2002**, *14*, 400−406. (n) Devlin, F. J.; Stephens, P. J.; Oesterle, C.; Wiberg, K. B.; Cheeseman, J. R.; Frisch, M. J. *J. Org. Chem.* **2002**, *67*, 8090−8096. (o) Stephens, P. J. Vibrational Circular Dichroism Spectroscopy: A New Tool for the Stereochemical Characterization of Chiral Molecules. In *Computational Medicinal Chemistry for Drug Discovery*; Bultinck, P., de Winter, H., Langenaecker, W., Tollenaere, J., Eds.; Dekker: New York, 2003; Chapter 26, pp 699−725. (p) Cerè, V.; Peri, F.; Pollicino, S.; Ricci, A.; Devlin, F. J.; Stephens, P. J.; Gasparrini, F.; Rompietti, R.; Villani, C. *J. Org. Chem.* **2005**, *70*, 664−669. (q) Stephens, P. J.; McCann, D. M.; Devlin, F. J.; Flood, T. C.; Butkus, E.; Stoncius, S.; Cheeseman, J. R. *J. Org. Chem.* **2005**, *70*, 3903−3913. (r) Devlin, F. J.; Stephens, P. J.; Besse, P. *Tetrahedron: Asymmetry* **2005**, *16*, 1557−1566. (s) Devlin, F. J.; Stephens, P. J.; Bortolini, O. *Tetrahedron: Asymmetry* **2005**, *16*, 2653−2663.

visible−near-UV transparent spectral region (i.e., excluding wavelengths at which electronic absorption and ECD occur). A prior example has been provided by 3-oxabicyclo[4.3.1]-decane-2,8-dione, **30**.[69] These molecules contradict the work of Rosini and co-workers,[70] who assert that, even if the predicted [α] value is incorrect in sign at long wavelengths, the predicted sign becomes correct as the wavelength decreases, approaching the longest wavelength absorption band. On that basis, it was claimed that, by using the dispersion of the OR instead of a single wavelength [α] value distant from electronic absorption, the assignment of ACs becomes "simple and reliable". Our prior work on **30**, and now, apparently, our work on **28**, shows that the assertions of Rosini and co-workers are not correct: just as sign errors can occur at long wavelengths, they can also continue to shorter wavelengths, becoming increasingly large in magnitude. Rosini and co-workers based their conclusions on the expectations that as the wavelength decreases [α] is increasingly dominated by the contribution of the lowest energy excitation and that the rotational strength of this excitation must be correctly predicted by TDDFT. Neither of these assumptions are universally correct. In the case of alkenes, [α] is the sum of many contributions of both signs, even at near-UV wavelengths. In addition, as we have shown in this work, predicted ECD spectra of the lowest energy excitations are not guaranteed to be in perfect agreement with experiment. In the case of **30**, we showed that not only are predicted [α] values uniformly opposite in sign to experimental values, but so also is the rotational strength of the lowest energy excitation, the n → π^* excitation of the carbonyl group. While, unquestionably, the more wavelengths that are used for comparing calculated and experimental rotations, the more reliable the AC deduced thence, it cannot be assumed that by so doing ACs of guaranteed reliability are assured.

While studying the carenes **7** and **8**, we have also studied the *trans* isomer of **8**, **29**. In contrast to **7** and **8** we have found two conformations of **29**, **a** and **b**, differing in energy/free energy by 0.64/0.56 kcal/mol. As with **28**, therefore, prediction of specific rotations requires conformational averaging. As with **28**, $[\alpha]_D$ values of **a** and **b** have the same sign and the sign of the predicted $[\alpha]_D$ is independent of the magnitudes of the conformational populations. In contrast to **28**, the predicted sign is the same as that of the experimental $[\alpha]_D$. Quantitatively, calculated and experimental $[\alpha]_D$ values differ by 107.8, a little greater than the largest deviation found for molecules **1**−**26** (94.5). This error could reflect an overestimate of the population of conformation **b** whose $[\alpha]_D$ value is approximately twice that of **a**. Examination of the variation in energy of **29** with respect to the dihedral angle C1C2C3C4 (Figure 16) shows however that the barrier between **a** and **b** is very small and the assumption that **29** is confined to the geometries of conformations **a** and **b** may be inadequate. To examine the consequences of large-amplitude motion along the coordinate C1C2C3C4, we have calculated the variation of $[\alpha]_D$ with respect to this coordinate and obtained a Boltzmann-averaged $[\alpha]_D$. While $[\alpha]_D$ is a rapidly varying function of C1C2C3C4, the result obtained is very close to that obtained assuming an equilibrium of two conformations. This may indicate that the latter assumption is valid, or that quantum-mechanical vibrational averaging is required instead of our classical averaging procedure.

Conclusion

Until now, the majority of studies of the reliability of TDDFT calculations of OR and ECD have focused on one molecule or a very few molecules. As a result, conclusions drawn from such studies have little statistical significance. Consequently, in determining the AC of a molecule whose AC is completely unknown, it has been difficult to evaluate the reliability of the AC arrived at. Most uses of TDDFT calculations for this purpose have simply ignored the issue.

We believe that this situation is not satisfactory and that much greater effort must be devoted to defining the reliabilities of TDDFT calculations of OR and ECD so that the reliabilities of ACs determined using such calculations can be quantitatively assessed. Since the electronic spectra of molecules depend on their functional groups, and the reliability of TDDFT calculations of electronic excitations is not necessarily uniform, we are approaching this issue one functional group at a time. We have recently reported our results for chiral alkanes.[6] Here, we are reporting our results for chiral alkenes.

Calculations of $[\alpha]_D$ for 26 conformationally rigid chiral alkenes using the TDDFT/GIAO methodology at the B3LYP/aug-cc-pVDZ//B3LYP/6-31G* level give results deviating on average from experimental $[\alpha]_D$ values by 28.7. Overall, the agreement between calculated and experimental $[\alpha]_D$ values is excellent. Undoubtedly, the TDDFT/GIAO methodology at this level describes the physics of optical rotation very reliably. Nevertheless, for reasons we have discussed in detail, calculations are not of 100% accuracy, and *this must be recognized in applications of TDDFT calculations to determining ACs*. We have presented a method by which it can be established whether an AC is or is not of 95% reliability (or any other percent reliability selected).

For a few molecules we have also predicted specific rotations for a range of visible−near-UV wavelengths. We have also studied two molecules which are conformationally flexible. In the case of 3-*tert*-butylcyclohexene, **28**, calculated specific rotations are of opposite sign compared to experimental values from 589 to 365 nm. While it is possible that the AC of **28** has been incorrectly assigned, at present it appears that **28** provides another example where TDDFT rotations are of incorrect sign. Further studies of **28** are warranted.

The situation with TDDFT ECD spectra is less straightforward. Over the experimentally accessible wavelength range, the electronic spectrum of an alkene is a highly complex mixture of valence and Rydberg excitations and is often strongly perturbed by solvents. Our predictions of the ECD spectra of eight conformationally rigid molecules, again at the B3LYP/aug-cc-pVDZ//B3LYP/6-31G* level, give very variable agreement with experimental spectra. It is clear that further improvements in the theoretical methodology are required before calculations of ECD spectra of alkenes can be routinely and reliably used in determining ACs.

(69) Stephens, P. J.; McCann, D. M.; Devlin, F. J.; Flood, T. C.; Butkus, E.; Stoncius, S.; Cheeseman, J. R. *J. Org. Chem.* **2005**, *70*, 3903−3913.
(70) Giorgio, E.; Viglione, R. G.; Zanasi, R.; Rosini, C. *J. Am. Chem. Soc.* **2004**, *126*, 12968−12976.
(71) Grimme, S.; Waletzke, M. *J. Chem. Phys.* **1999**, *111*, 5645−5655.
(72) Diedrich, C.; Grimme, S. *J. Phys. Chem. A* **2003**, *107*, 2524−2539.
(73) Stephens, P. J.; Devlin, F. J.; Aamouche, A. In *Chirality: Physical Chemistry*; Hicks, J. M., Ed.; ACS Symposium Series; American Chemical Society: Washington, DC, 2002; Vol. 810, pp 18−33.
(74) Pedersen, T. B.; Koch, H. *J. Chem. Phys.* **2000**, *112*, 2139−2147.
(75) Harada, N.; Nakanishi, K. *Circular Dichroic Spectroscopy − Exciton Coupling in Organic Chemistry*: University Science Books: Mill Valley, CA, 1983; pp 304−306.

Acknowledgment. We are grateful for financial support from the National Science Foundation (to P.J.S., Grant CHE-0209957). We also thank the USC High Performance Computing and Communication (HPCC) facility for computer time, Dr. J. R. Cheeseman of Gaussian Inc. for his continual assistance and advice, and Prof. J. Autschbach for discussions regarding *trans*-cyclooctene.

Supporting Information Available: Calculated geometries, PES scans, optical rotations, excitation energies, oscillator strengths, rotational strengths, and ECD spectra and experimental geometries, optical rotations, and UV spectra. This material is available free of charge via the Internet at http://pubs.acs.org.

JO060755+